EXPERIMENTAL INVESTIGATION OF FAILURE IN THIN RINGS SUBJECTED TO UNIFORM EXTERNAL PRESSURE

Jules Henry Demyttenaere
and
William Joseph Norris

EXPERIMENTAL INVESTIGATION OF FAILURE IN THIN RINGS SUBJECTED TO UNIFORM EXTERNAL PRESSURE

by

JULES HENRY DEMYTTENAERE, LTJG., U.S.NAVY
B.S., United States Naval Academy
(1949)

ENT OF THE

REE OF

Letter on front cover:

EXPERIMENTAL INVESTIGATION OF
FAILURE IN THIN RINGS SUBJECTED
TO UNIFORM EXTERNAL PRESSURE

ECHNOLOGY

JULES HENRY DEMYTTENAERE
and
WILLIAM JOSEPH NORRIS

Letter on front cover:

EXPERIMENTAL INVESTIGATION OF
FAILURE IN THIN RINGS SUBJECTED
TO UNIFORM EXTERNAL PRESSURE

JULES HENRY DEMYTTENAERE
and
WILLIAM JOSEPH NORRIS

'IGATION OF FAILURE IN THIN

'FORM EXTERNAL PRESSURE

.AERE, LTJG., U.S.NAVY
cates Naval Academy
(1949)

and

WILLIAM JOSEPH NORRIS, LTJG., U.S.NAVY
B.S., United States Naval Academy
(1949)

SUBMITTED IN PARTIAL FULFILLMENT OF THE

REQUIREMENTS FOR THE DEGREE OF

NAVAL ENGINEER

at the

MASSACHUSETTS INSTITUTE OF TECHNOLOGY

May, 1954

EXPERIMENTAL INVESTIGATION OF FAILURE IN THIN RINGS SUBJECTED TO UNIFORM EXTERNAL PRESSURE

by

JULES HENRY DEMYTTENAERE, LTJG., U.S.NAVY
B.S., United States Naval Academy
(1949)

TITLE: EXPERIMENTAL INVESTIGATION OF FAILURE IN THIN RINGS SUBJECTED TO UNIFORM EXTERNAL PRESSURE

AUTHORS: J. H. Demyttenaere, LTJG., U.S.N., and
W. J. Norris, LTJG., U.S.N.

Submitted to the Department of Naval Architecture and Marine Engineering on May 24, 1954, in partial fulfillment of the requirements for the degree of Naval Engineer.

ABSTRACT

The object of this thesis was to investigate experimentally the strain distributions and ultimate failures in thin circular and non-circular aluminum rings subjected to uniform external pressure.

A test apparatus was designed to permit the application of hydraulic pressure to the outer circumference of a ring placed between two sheets of Plexiglas. The small clearance between the edges of the ring and the Plexiglas was sealed by a continuous rubber gasket of slightly greater width fitted around the outer circumference of the ring. Except for friction at the gasket-Plexiglas interface, the ring was free of restraint.

Nine rings of aluminum alloy, 61S-T6, were tested to collapse; the variable in this series was out-of-roundness. Correlation between measured and predicted strains was obtained in five of the six rings in which the assumptions of the prediction were valid. A somewhat arbitrary strain distribution was observed in the two most circular rings. The four rings of moderate out-of-roundness collapsed very near predictions based upon a criteria related to the maximum stress level in the outer fibers while the three rings of relatively large out-of-roundness failed at pressures somewhat higher than predicted. The two most circular rings collapsed near a computed pressure when the minimum rather than average section thickness was used in the calculation. Collapse pressures were predicted most accurately when the stress used in conjunction with the failure criteria was defined by the point on the stress-strain curve at which marked non-linearity occurred.

An analysis of the results indicates that strain distributions in an out-of-round ring loaded by uniform external pressure can be predicted with satisfactory

TITLE: [illegible]

AUTHORS: [illegible]

[illegible]

accuracy provided the assumptions made in the prediction are satisfied; namely, that the thickness to diameter ratio be the order of 0.0285 and that the initial configuration assumed is actually predominate. A failure criteria based upon the stress level in the outer fibers will, when the assumptions above are fulfilled, predict collapse quite accurately in rings of out-of-roundness to thickness ratio between 0.10 and 0.30. At larger values of out-of-roundness the criteria is conservative but not over cautious.

It is recommended that the experimentation be extended to include a quantitative investigation of the effects of deviations from a basic two lobe out-of-roundness such as might be obtained in a practical situation. Such an investigation should be conducted using rings of constant thickness in order to avoid many of the unnecessary complications encountered in the analysis of data obtained in this thesis.

Cambridge, Massachusetts
May 24, 1954

Professor Leicester F. Hamilton
Secretary of the Faculty
Massachusetts Institute of Technology
Cambridge, Massachusetts

Dear Sir:

In accordance with the requirements for the degree of Naval Engineer, we submit herewith a thesis entitled, "Experimental Investigation of Failure in Thin Rings Subjected to Uniform External Pressure."

ACKNOWLEDGMENTS

The authors wish to express their appreciation to those individuals at the Massachusetts Institute of Technology, Boston Naval Shipyard, and the David Taylor Model Basin, who so generously gave their time and advice so that the objectives of this thesis might be accomplished.

Specifically the authors wish to thank Dr. E. Wenk, Jr., of the David Taylor Model Basin, who originally posed many of the problems involved; Dr. W. W. Murray, of the Massachusetts Institute of Technology, and his assistant Mr. Peter Stein for their most helpful advice on a multitude of details.

The authors are particularly grateful to their Thesis Supervisor, J. H. Evans, Assistant Professor of Naval Architecture, Massachusetts Institute of Technology, for his encouragement and advice during the progress of the thesis.

ACKNOWLEDGMENTS

The authors wish to express their appreciation to those civilians at the Massachusetts Institute of Technology, Boston Naval Shipyard, and the David Taylor Model Basin, who so generously gave their time and advice so that the objectives of this thesis might be accomplished.

Specifically the authors wish to thank Dr. B. Yeh, Jr., of the David Taylor Model Basin, who originally posed [illegible] involved; Lt. W. Murry, of the [illegible] Institute of Technology, and his assistant Mr. Peter Dodd for their most helpful advice on a multitude of problems.

The authors are particularly grateful to their thesis supervisor, A. R. Kuhn, Assistant Professor of Naval Architecture, Massachusetts Institute of Technology, for his encouragement and [illegible] the preparation of the thesis.

SYMBOLS AND ABBREVIATIONS

The following symbols and abbreviations are used throughout this report:

b = Width of ring, in inches

D = Mean diameter measured to neutral axis, in inches

E = Modulus of elasticity - initial slope of stress-strain curve, psi.

ε = Compressive strain, inches/inch or micro-inches/inch.

h = Thickness of ring, in inches.

I = Moment of inertia of ring cross-section about neutral axis, in $in.^4$

P = Pressure, psi.

$P_{crit.}$ = Collapse pressure of a circular ring, psi.

psi. = Pounds per square inch.

R = Mean radius to neutral axis of ring, in inches.

R_o = Mean radius to outer circumference of ring, in inches.

σ = Compressive stress, psi.

σ_y = 0.2% proof stress, psi.

θ = Angular coordinate to designate positions on ring, in degrees.

u_o = Two-lobe out-of-roundness, maximum deviation from a true circle of the same perimeter as the two-lobe configuration, in inches.

u_1 = Three-lobe out-of-roundness, inches

u_2 = Four-lobe out-of-roundness, inches

SYMBOLS AND ABBREVIATIONS

The following symbols and abbreviations are used throughout this report:

b = Width of "n", in inches

D = Mean diameter measured to centers of n's, in inches

E = Modulus of elasticity - initial slope of stress-strain curve, psi.

ϵ = Compressive strain, inches/inch or micro-inches/inch.

n = Thickness of rim, in inches.

I = Moment of inertia of ring cross-section about neutral axis, in $in.^4$

P = Pressure, psi.

$P_{crit.}$ = Collapse pressure of a circular rim, psi.

psi. = Pounds per square inch.

R = Mean radius to neutral axis of rim, in inches.

R_o = Mean radius to outer circumference of ring, in inches.

σ = Compressive stress, psi.

σ_y = 0.2% proof stress, psi.

θ = Angular coordinate to describe position on rim, in degrees.

n_2 = Two-lobe out-of-roundness, maximum deviation from a true circle of the same circumference as the two-lobe configuration, in inches.

n_3 = Three-lobe out-of-roundness, inches.

n_4 = Four-lobe out-of-roundness, inches.

Experimental Investigation of Failure in Thin Rings Subjected to Uniform External Pressure

TABLE OF CONTENTS

TABLE OF CONTENTS

TABLE OF CONTENTS (Continued)

TABLE OF CONTENTS (cont'd)

I.

INTRODUCTION

Objective

The objective of this thesis is to investigate experimentally the strain distributions and ultimate failures obtained in thin circular and non-circular aluminum rings subjected to uniform external pressure.

Background

The slender column in axial compression is generally cited as the classic example of a buckling failure. The behavior of such axially loaded columns was subjected to an early theoretical analysis, and at the same time numerous investigators supplied experimental data relevant to the problem. The experimentation served two purposes. First, the conclusions substantiated the basic concepts and accuracy of the theoretical analysis. Second, certain practical aspects of the problem were magnified. Thus, through an analysis of experimental data and an appreciation of the difficulty in obtaining a perfectly loaded column, Moncrieff (1) was able to propose a practical criteria for column strength which included the assumption of an inherent eccentricity.

The failure of thin rings subjected to uniform external pressure is analogous to the buckling of columns.

I.

INTRODUCTION

Objective

The objective of this thesis is to investigate experimentally the strain distributions and ultimate failures obtained in thin circular and non-circular aluminum rings subjected to uniform external pressure.

Background

The slender column in axial compression is generally cited as the classic example of a buckling failure. The behavior of such axially loaded columns was subjected to an early theoretical analysis, and in the same time numerous investigators supplied experimental data relevant to the problem. The experimentation served two purposes. First, the conclusions subjected the axial concept and accuracy of the theoretical analyses. Second, certain practical aspects of the problem were clarified. Thus, through an analysis of experimental data and a realization of the difficulty in obtaining perfectly loaded column, Bonnerait [illegible] criteria for column strength [illegible] of an ideal perfect column.

The failure of thin rings [illegible] external pressure is [illegible].

The buckling of such uniformally loaded rings has been treated theoretically by investigators as early as Levy (2) and as recent as Boresi (3). In addition a clear presentation of the problem is given by Timoshenko (4). Despite the extensive theoretical analysis, experimentation has been lacking. In a search of the literature, the authors found no instance of a ring being collapsed experimentally under a uniform external load.

The lack of experimental data relative to the ring problem may be partially explained by the following:

1. The use of the ring as a structural member is not so widespread as the column. Hence the need for usable data was not pressing.
2. Many of the conclusions formulated as a result of column analysis were applicable to the ring problem.
3. The buckling of a cylinder subjected to external pressure is closely related to the buckling of a ring. Obviously much of the data gleaned from failure of cylinders also applies to rings. The collapse of a cylinder may be effected simply and conveniently in the laboratory.
4. A free ring loaded with uniform external pressure offers a difficult problem in the design of a test apparatus.

The buckling of such uniformly loaded rings has been treated theoretically by investigators as early as Levy (2) and as recent as Borsel (3). In addition a clear presentation of the problem is given by Timoshenko (4). Despite the extensive theoretical analysis, experimentation has been lacking. In a search of the literature, the authors found no instance of a ring being collapsed experimentally under a uniform external load.

The lack of experimental data relative to the ring problem may be partially explained by the following:

1. The use of the ring as a structural member is not so widespread as the column. Hence the need for usable data was not pressing.
2. Many of the conclusions formulated as a result of column analysis were applicable to the ring problem.
3. The buckling of a cylinder subjected to external pressure is closely related to the buckling of a ring. Obviously much of the data gleaned from failure of cylinders also applies to rings. The collapse of a cylinder may be effected simply and conveniently in the laboratory.
4. A free ring loaded with uniform external pressure offers a [illegible] in the design of [illegible] test apparatus.

Despite the apparent validity of the theoretical analysis of ring buckling and the availability of related experimental data, there is a need for experimentation devoted specifically and directly to the collapse of a thin ring. This need arises not merely from the satisfaction to be gained by proving the validity of the concepts or assumptions of the pertinent theory but from a desire to obtain a practical perspective. Thus, some peculiarity of the ring problem may yet be unrecognized; practical expedients such as the assumption of an inherent out-of-roundness may be necessary. Furthermore, there is need for a substantial and tested criteria of failure which may or may not be related to the stress level at the inner or outer surface of the ring. It is to be appreciated that in out-of-round rings, failure results when stable equilibrium is not possible between an internal and external bending moment and is not a direct result of some specified stress in the outer fibers. In addition, the ring provides a convenient means of studying and evaluating out-of-roundness not only in rings but also in cylinders. In a theoretical approach out-of-roundness may be represented very simply by a Fourier series; there is need for a simple, yet reliable, measure of out-of-roundness which has a practical value.

Problem

The authors have undertaken the task of obtaining and

Problem

The authors have interpreted the lack of obtaining a measure of out-of-roundness which has a practical value. Fourier series; there is need for a simple, yet reliable, out-of-roundness may be represented very simply by a in rings but also in cylinders. In a theoretical exposition means of studying and evaluating out-of-roundness not only outer fibers. In addition, the ring provides a convenient and is not a direct result of some specified stress in the possible between an internal and external bending moment rings, failure results when stable equilibrium is not the ring. It is to be appreciated that in out-of-round lated to the stress level at the inner or outer surface of and tested criteria of failure which may or may not be re- be necessary. Furthermore, there is need for a substantial ever as the assumption of an inherent out-of-roundness may the ring problem may yet be unrecognized; practical experience obtain a practical perspective. Thus, some peculiarity of or assumptions of the pertinent theory out from a desire to tion to be gained by proving the validity of the concepts thin ring. This need arises not merely from the satis- devoted specifically and directly to the collapse of a experimental data, there is a need for experimentation analysis of ring buckling and the availability of related Despite the apparent validity of the theoretical

evaluating experimental data of the type referred to above.

Implied in this assignment are the following specific problems:

1. The design and construction of a test apparatus which will permit the application of a uniform external load to an essentially free ring.
2. The instrumentation of a ring such that the strain distribution may be determined.
3. A comparison of measured strain distribution and failure loads with theoretical predictions.
4. A review of experimental results for the purpose of pointing out the practical aspects of the ring buckling problem.

evaluating experimental data of the type required to study.

Implied in this assignment are the following specific problems:

1. The design and construction of a test apparatus which will permit the application of a uniform external load to an eccentrically fire ring.
2. The instrumentation of a ring such that the strain distribution may be determined.
3. A comparison of measured strain distribution and failure loads with theoretical predictions.
4. A review of experimental results for the purpose of pointing out the practical aspects of the ring buckling problem.

II.

PROCEDURE

Outline

The procedure followed in this thesis is to be presented under the following subheadings:

(a) Selection of Material for Construction of Rings

(b) Manufacture of Rings

(c) Ring Dimensions and Instrumentation

(d) Design and Manufacture of Test Apparatus

(e) Proof Test of Apparatus

(f) Test of Rings

(g) Test of Compression Specimens

(h) Evaluation of Data

(i) Correlation of Data

II.

PROCEDURE

Outline

The procedure followed in this thesis is to be presented under the following subheadings:

(a) Selection of Material for Construction of Rings

(b) Manufacture of Rings

(c) Ring Dimensions and Instrumentation

(d) Design and Manufacture of Test Apparatus

(e) Proof Test of Apparatus

(f) Test of Rings

(g) Test of Compression Specimens

(h) Evaluation of Data

(i) Correlation of Data

Selection of Material for Construction of Rings

Rings were machined from a length of 9" aluminum alloy (61S-T6)tubing of 1/4" wall thickness. The actual outside diameter as determined by the authors was 9.016".

The decision to use aluminum alloy test rings was based upon the following considerations:

1. To properly correlate measured and predicted strain distributions it was necessary to select a material in which the stress-strain relationship was essentially linear over a considerable range of stress. Aluminum alloy 61S-T6 was suitable in this respect since the estimated 0.2% proof stress was 40,000 psi. (5).
2. The predicted failure pressures for rings of reasonable diameter and thickness were satisfactory. Reasonable dimensions were defined as any diameter and thickness of tubing or pipe which was available and which could be accommodated by the facilities in the testing laboratory. A relatively high failure pressure was desirable in that sufficient accuracy could be obtained without the use of an extremely sensitive pressure measuring device. Yet the maximum pressure should not be so high as to require an excessively complicated and expensive test apparatus.

Selection of Material for Construction of Rings

Rings were machined from a length of 5" aluminum alloy (6IS-T6)tubing of 1\4" wall thickness. The mutual outside diameter as determined by the authors was 9.016".

The decision to use aluminum alloy test rings was based upon the following considerations:

1. To properly correlate measured and predicted strain distributions it was necessary to select a material in which the stress-strain relationship was essentially linear over a considerable range of stress. Aluminum alloy 61S-T6 was suitable in this respect since the calculated 0.2% proof stress was 40,000 psi. (5).

2. The predicted failure pressures for rings of reasonable diameter and thickness were satisfactory. Reasonable dimensions were defined as any diameter and thickness of tubing or pipe which was available and which could be accommodated by the facilities in the testing laboratory. A total axial pressure of 1,000 psi was considered sufficient accuracy could be obtained without the use of an extremely sensitive pressure measuring device. Yet the maximum pressure would not be so high as to induce an excessively large stress in the test ring.

Manufacture of Rings

The aluminum alloy tubing as received was cut into sections of 2 1/2" to 3 1/2" lengths. Out-of-roundness was then intentionally introduced in the majority of these pieces by placing the individual sections in a loading machine and applying a load. When the desired permanent set had been obtained the load was removed. Since essentially circular rings were to be machined from the remainder of the sections no deformation was introduced. In this manner a range of out-of-roundness was obtained which varied from u_o = 0.007" in the tubing as received to u_o = 0.296" in the section with the greatest intentional deformation.

As a result of the permanent set imposed, there existed an unknown residual stress at points stressed above the elastic limit. To insure linearity of measured strains over a maximum range, the sections were subjected to a solution heat treatment followed by the precipitation heat treatment required to obtain alloy 61S-T6. Uniformity of properties was insured by heat treating, as a group, all sections plus the material from which compression specimens were to be manufactured.

Wooden plugs about 1 inch in thickness were tailored to fit into one end of each section in order to facilitate final machining and to avoid distortion caused by the clamping jaws of the lathe. Rings of specified width were

Manufacture of Rings

The aluminum alloy tubing as received was cut into sections of 2 1/2" to 3 1/2" lengths. Out-of-roundness was then intentionally introduced in the majority of these pieces by placing the individual sections in a loading machine and applying a load. When the desired permanent set had been obtained the load was removed. Since essentially circular rings were to be machined from the remainder of the sections no deformation was introduced. In this manner a range of out-of-roundness was obtained which varied from w_o = 0.007" in the tubing as received to w_o = 0.250" in the section with the greatest intentional deformation.

As a result of the permanent set imposed, there existed an unknown residual stress at points stressed above the elastic limit. To insure linearity of measured strains over a maximum range, the sections were subjected to a solution heat treatment followed by the precipitation heat treatment required to obtain alloy 61S-T6. Uniformity of properties was insured by heat treating, as a group, all sections from the material from which compression specimens were to be manufactured.

Wooden plugs about 1 inch in thickness were tailored to fit into one end of each section in order to facilitate final machining and to avoid distortion caused by the clamping jaws of the lathe. Light [illegible] were

then cut from the sections; this width was determined by a direct measurement of the clearance between the surfaces of the annular test chamber in the completed test apparatus. The rings as cut were generally 0.444" to 0.446" in width, the maximum deviation for a single ring being 0.001". The thickness of the rings remained the same as received.

Ring Dimensions and Instrumentation

The outside diameter of each ring was found by fitting a wire 0.01" in diameter around the outer circumference. The wire was scribed and then measured between the scribe marks on a 36" steel rule. An outside radius was computed by dividing the measured circumference by 2π and correcting for the thickness of the measuring wire. All radii thus determined were averaged to give a mean outside radius (4.508") for use in the computations.

The measuring wire was scribed at intervals of 30 degrees of arc length and again fitted around each ring. The scribe marks were transferred to the aluminum alloy. For those rings in which deformation had been introduced care was taken to locate one of the scribe marks as close as possible to the point of maximum diameter. The twelve stations so determined were designated 0° through 330° in 30° increments, with 0° at a point of maximum diameter. The thickness and width at each station were measured with small micrometers

Ring Dimensions and Instrumentation

The outside diameter of each ring was found by first
a wire 0.01" in diameter around the outer circumferen-
The wire was scribed and then measured between the scrib
marks on a 36" steel rule. An outside reading was compute
by dividing the measured circumference of 3.14 and correc-
ing for the thickness of the measuring wire. All result
thus determined were averaged to give a mean outside radius
(4.503") for use in the computations.

The measuring wire was scribed at intervals of 90 degr
of arc length and again after rotating each ring. The centra
marks were transferred by the "universal micro alloy". For those
rings in which deformation had been induced data was t
to locate one of the scribe marks as close as possible to
the point of maximum diameter. The twelve diameters
sired were designated 0°, [illegible] in the clockwise
with 0° at a point of maximum diameter. The thickness
width at each station were measured with small micrometer
the maximum deviation for a single ring being 0.001".
The rings as cut were generally 0.444" to 0.446" in width,
of the annular test chamber in the completed test apparatus.
A direct measurement of the clearance between the surfaces
then cut from the sections; this width was determined by

while the outside diameter was measured at stations and half stations with large outside micrometers.

Baldwin SR-4, type A-7, strain gages were cemented to the inner surface of the ring at each station with the gage length along the circumference. Photograph No. 1 shows the strain gages in position on the ring after the leads had been soldered in place. The leads were passed through the bottom of the test apparatus and connected to the multiple selector switchbox which in turn was connected to the strain indicator. The dummy gage was attached to a scrap piece of aluminum alloy which was placed in the vicinity of the test apparatus. Leads from the dummy were connected to the switchbox.

Design and Manufacture of Test Apparatus

The design of the apparatus and its associated equipment can be understood from photographs Nos. 2, 3, 4 and Figures I and II. The bucket pump had been previously tested up to a pressure of 1600 psi and was considered to be of sufficient capacity to supply oil to the pressure chamber enclosing the ring.

The test apparatus was made by the Mechanical Engineering Department machine shop at the Massachusetts Institute of Technology to plans and specifications furnished by the authors. It is to be noted that provision was made for a

while the outside diameter was measured at stations and bet-
stations with large outside micrometers.

Baldwin SR-4, type A-7, strain gages were cemented to the inner surface of the ring at each station with the gage length along the circumference. Photograph No. 1 shows the strain gages in position on the ring after the leads had been soldered in place. The leads were passed through the bottom of the test apparatus and connected to the multiple selector switchbox which in turn was connected to the strain indicator. The dummy gage was attached to a scrap piece of aluminum alloy which was placed in the vicinity of the test apparatus. Leads from the dummy were connected to the switchbox.

Design and Manufacture of Test Apparatus

The design of the apparatus and its associated equipment can be understood from photographs Nos. 2, 3, 4 and Figures I and II. The bucket pump had been previously tested up to a pressure of 1500 psi and was considered to be of sufficient capacity to supply oil to the pressure chamber enclosing the ring.

The test apparatus was made by the Mechanical Engineering Department machine shop at the Massachusetts Institute of Technology to plans and specifications furnished by the authors. It is to be noted that provision was made for a

Photograph No. 1

RING WITH STRAIN GAGES AND LEADS

Photograph No. 2

TEST APPARATUS

Photograph No. 3

TEST APPARATUS

Photograph No. 4

TEST APPARATUS WITH CATHETOMETER MOUNTED

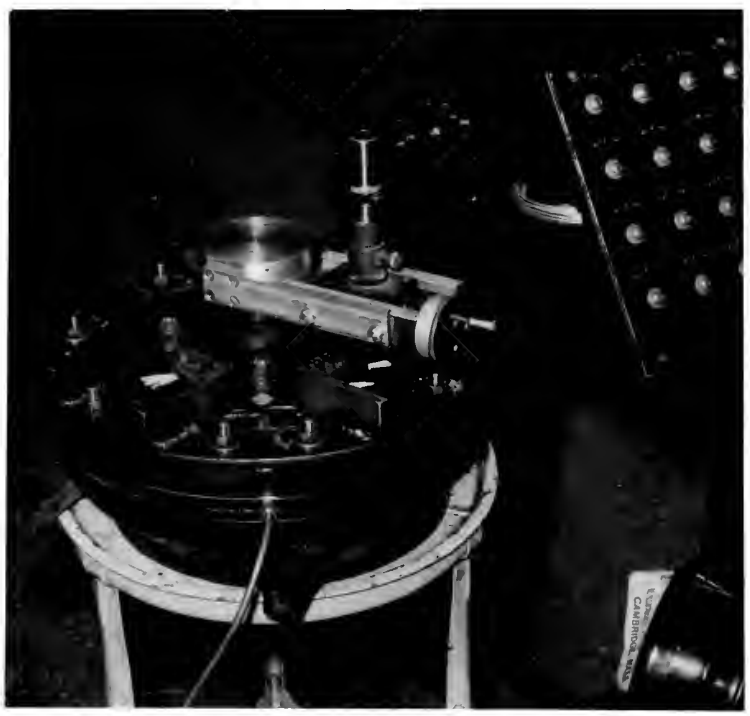

FIGURE I

TEST APPARATUS

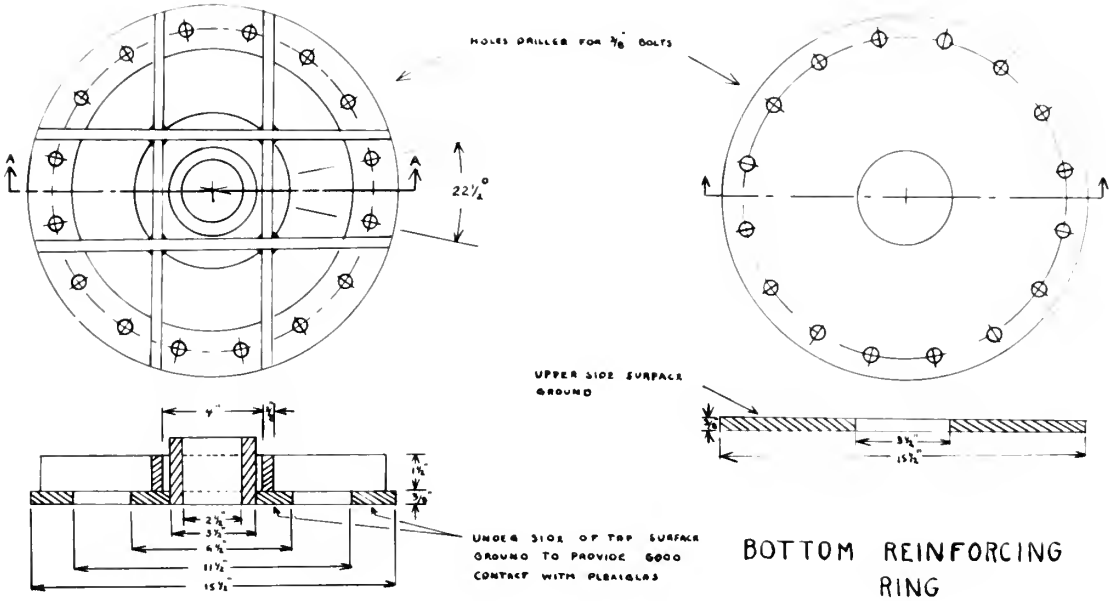

TOP ASSEMBLY

BOTTOM REINFORCING RING

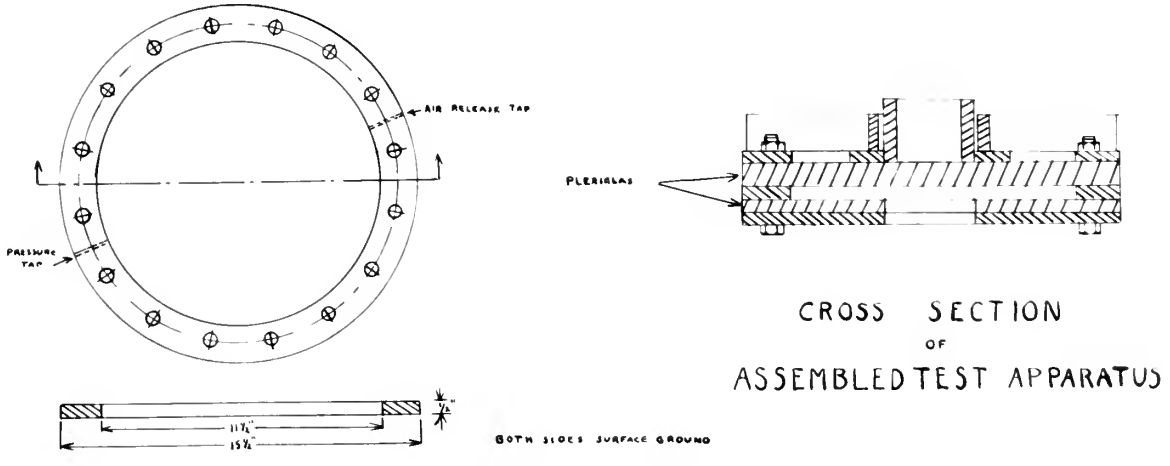

SPACER RING

CROSS SECTION OF ASSEMBLED TEST APPARATUS

4/13/54 YAU 2 97

FIGURE II

CATHETOMETER MOUNTING

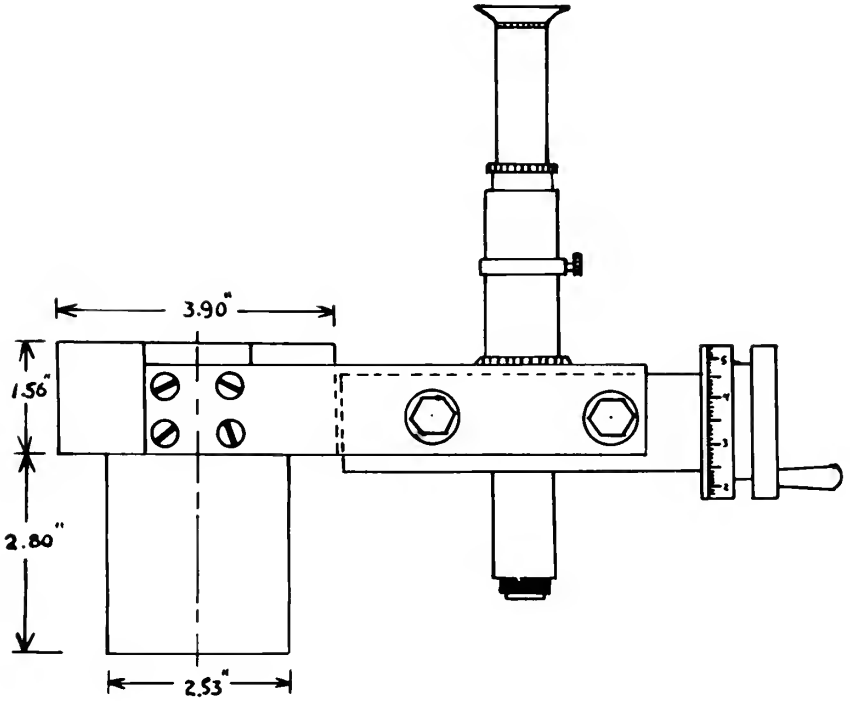

SIDE VIEW

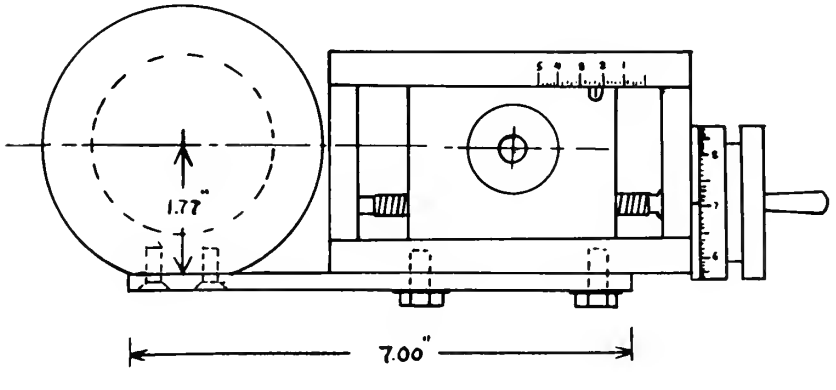

TOP VIEW

4/24/54 MD - WJM

viewing chamber which would permit inspection of the rings during application of pressure. The pressure gage was furnished by the Department of Mechanical Engineering, MIT, and calibrated by the authors.

Proof Test of Apparatus

Upon completion of the test chamber by the machine shop, the complete test apparatus as indicated in Photographs Nos. 2, 3, and 4 was assembled and proof tested by the authors. Two preliminary test rings were machined from a section of the original aluminum tubing for use in this phase of the testing.

To maintain pressure in the test chamber behind the aluminum rings, a gasket of width slightly greater than 1/2" was placed around the outer circumference of the ring; several types of gasket material were tried. In each case the gasket material was cut to size, glued to the outer surface of the ring, and bound lightly by several strands of light string lying along the circumference. The ring was then placed in the test apparatus and the upper Plexiglas surface and top web assembly were bolted down. Oil was pumped into the test chamber with the bucket pump and the air vented through the air release tap. Pressure was built up behind the ring in the test chamber until, in most cases, the gasket material extruded between the Plexiglas surfaces

and the edges of the ring. As a result of these trials, the best gasket material for sealing the ring edges appeared to be a rubber gasket cut from an ordinary truck tire inner tube approximately 9" in diameter. This type of gasket was used throughout the remainder of the proof tests and the final tests. Pressures up to 875 psi. were maintained in the test chamber using this gasket.

An Ames dial gage was mounted on the steel web assembly midway between the top inner and outer backing up rings to determine the maximum deflection of the Plexiglas surface as pressure was applied. A maximum deflection of 0.007" occurred at 875 psi. The deflection occurring at 500 psi. was of the order of 0.004".

It became apparent during these tests that some type of lubricant was necessary to eliminate or reduce to a minimum the friction between the rubber gasket and the Plexiglas surfaces. Several types of lubricant were tried and the best found to be black rubber-to-metal cement. Strains at a particular station were found to vary with the lubricant and gasket material when the same pressure was applied.

The cathetometer was mounted during the preliminary test phase and attempts were made to take deflection readings. Unfortunately the cathetometer proved impractical as a means

of reading deflection for several reasons, viz.

1. The slight deflection of the upper Plexiglas surface distorted the ring as seen through the eye piece of the cathetometer.
2. The use of black rubber-to-metal cement as a lubricant obscured the aluminum ring in the test chamber when oil was introduced.

The proof testing period was of infinite value to the authors in planning and carrying out the final tests of the circular and non-circular rings.

Test of Rings

One result of the proof testing was the formulation of a standard test procedure. As a consequence, the remainder of the tests were made in a minimum amount of time and with little difficulty.

Nine rings were tested in accordance with the following steps:

1. Leads were soldered to strain gages, threaded through the bottom of the test chamber, and connected to terminals on the back of the multiple selector switchbox.
2. Black rubber-to-metal cement was applied to the rubber gasket and outer circumference of the ring. (Cement allowed to dry 3-5 minutes).
3. The rubber gasket was slipped around the outer

of reading deflection for several reasons, viz.

1. The slight deflection of the outer flexible surface distorted the ring as seen through the eye piece of the cathetometer.

2. The use of black rubber-to-metal cement as a lubricant obscured the aluminum ring in the test chamber when oil was introduced.

The proof testing period was of infinite value to the authors in planning and carrying out the final tests of the circular and non-circular rings.

Test of Rings

One result of the proof testing was the formulation of a standard test procedure. As a consequence, the remainder of the tests were made in a minimum amount of time and with little difficulty.

Nine rings were tested in accordance with the following steps:

1. Leads were soldered to shrink rings, threaded through the bottom of the test chamber, and connected to terminals on the deck of the multiple selector switchbox.

2. Black rubber-to-metal cement was applied to the rubber gasket and outer circumference of the ring. (Cement allowed to dry 2-3 hrs.).

3. The rubber gasket [illegible]

circumference of the ring and secured in place by four strands of light string. The gasket was adjusted so that the bevels extended an equal distance beyond the edges of the ring.

4. A thin film of #40 S.A.E. motor oil was applied to the inner Plexiglas surfaces.
5. The ring was centered in the test chamber.
6. The upper Plexiglas plate was slipped over the bolts and held down firmly by hand while the top web assembly was lowered into place.
7. All bolts were tightened.
8. Initial zero readings were set on all strain gages by adjusting switchbox set screws.
9. Air was vented through the air release tap while the test chamber was being filled with oil from the bucket pump.
10. Pressure in the chamber was increased in increments of 50 to 100 psi. depending upon the expected collapse pressure of the particular ring, 100 psi. increments being used for the more circular rings and 50 psi. increments for the more out-of-round rings. Strain gage readings were taken at each pressure increment.
11. Because the collapse of the more circular rings occurred rather quickly, the pressure was maintained

circumference of the ring and secured in place by four strands of light string. The gasket was adjusted so that the bevels extended an equal distance beyond the edges of the ring.

4. A thin film of #40 S.A.E. motor oil was applied to the inner flexiglas surfaces.

5. The ring was centered in the test chamber.

6. The upper flexiglas plate was slipped over the bolts and held down firmly by hand while the top web assembly was lowered into place.

7. All bolts were tightened.

8. Initial zero readings were set on all strain gages by adjusting switchbox set screws.

9. Air was vented through the air release tap while the test chamber was being filled with oil from the pocket pump.

10. Pressure in the chamber was increased in increments of 50 to 100 psi, depending upon the expected collapse pressure of the particular ring, 100 psi. increments being used for the more circular rings and 50 psi. Increments for the more ~~t~~-of-round rings. Strain gage readings were taken at each pressure increment.

11. Because the collapse of the more circular rings occurred rather quickly, the pressure was [illegible]

momentarily at 5 psi. increments when the ring was near collapse. The collapse of a significantly out-of-round ring generally proceeded at a very slow rate. In this case the strain indicator was connected to read the maximum strain. Pressure was then increased in steps of 5 psi. or smaller, each pressure being maintained until the strain indication steadied.

12. When the strain indicator needle did not steady, failure occurred. Failures in the more circular rings were evidenced by an immediate drop in pressure and obvious deformations.

Collapse pressure was thus defined as that pressure at which static strains could not be maintained. Complete failure of all rings was characterized by large, visible deflections regardless of the rate at which collapse proceeded; once complete failure occurred the ring would not again sustain collapse pressure.

Test of Compression Specimens

The stress-strain curve for the material used in the fabrication of the rings for this investigation was determined by means of the "Single Thickness" compression test method. Three specimens of the aluminum alloy (61S-T6) were tested in the compression block as indicated in photographs Nos. 5 and 6. A complete description and

[illegible] the most [illegible] and [illegible].

[illegible] were tested in the compression [illegible]

[illegible] section. Three specimens of the [illegible] collapse

tested by means of the "Simple Thickness" compression test

fabric [illegible] of the rings [illegible]

momentarily [illegible] creasing [illegible]

wear collapse. The collapse of [illegible] very

out-of-round rung generally preceded by a very

slow rate. In this case the static load was

connected to a rod the maximum attained. Pressure was

then increased in steps of 5 per. or less, each

pressure being maintained until the [illegible] ceased

tion arrested.

IX. When the static indicator needle did not [illegible],

failure occurred. Failures in the whole circular

rings were evidenced by an immediate rise in

pressure and obvious deformations.

Collapse pressure was thus defined as that pressure

at which static stress could not be maintained. Complete

failure of all rings was characterized by large, visible

deflections regardless of the rate by which collapse proceeded;

once complete failure occurred the ring would not sustain

sustain collapse pressure.

Test of Compression Specimens

[illegible]

Photograph No. 5

HUGGENBERGER TENSOMETERS MOUNTED
ON SPECIMEN IN COMPRESSION BLOCK

Photograph No. 6

COMPRESSION BLOCK IN LOADING MACHINE

bibliography for this method is given in reference (6). Compression tests in general are also discussed in reference (5).

Evaluation of Data

All data obtained during the testing period can be grouped as follows:

1. Dimensions
2. Pressure at which strains were recorded
3. Pressure at which ring collapsed
4. Strain readings
5. Compression Specimen test data.

With one exception all dimensions recorded were taken with micrometers and can be considered accurate to 0.0005". The circumference, as determined by the scribed wire, was read to the nearest 1/128" on the steel rule. However, the authors felt that the accuracy was of the order of 1/64", one scale division. The accuracy of the average outside radius then becomes 0.0025".

The pressure gage was calibrated by the authors prior to the tests using a dead-weight tester. Two calibration runs were made using increasing pressures and two with decreasing pressures. The maximum deviation from true was found to be 4 psi.; the largest difference between an up reading and a down reading for the same true pressure was also 4 psi. Used in conjunction with a calibration curve

bibliography for this method is given in reference (6).

Compression tests in general are also discussed in reference (5).

Evaluation of Data

All data obtained during the testing period can be grouped as follows:

1. Dimensions
2. Pressure at which strains were recorded
3. Pressure at which ring collapsed
4. Strain readings
5. Compression Specimen test data.

With one exception all dimensions recorded were taken with micrometers and can be considered accurate to 0.0005". The circumference, as determined by the scribed wire, was read to the nearest 1/128" on the steel rule. However, the authors felt that the accuracy was of the order of 1/64", one scale division. The accuracy of the average outside radius then becomes +0.015".

The pressure [illegible] to the tests using a dead-weight tester. Two calibrations were made [illegible] pressures and the Mid- [illegible] pressure. The maximum deviation [illegible] from [illegible] to be 1 per cent. The largest difference [illegible]

the gage was considered to be accurate to ± 2 psi. althougn the accuracy was considerably better over most of the pressure range. During the tests the indicated pressure could be held fairly constant. An accuracy of plus or minus one half a scale division (±2 1/2 psi.) is probably conservative but will be assumed. The accuracy of the recorded pressures at which strain readings were taken then becomes ±5 1/2 psi.

With one additional consideration the above remarks also apply to the accuracy of the recorded collapse pressures. The collapse of rings with significant amounts of out-of-roundness occurred rather slowly. It would seem that the pressure could be inadvertently increased above the true collapse pressure, the only effect being an accelerated failure. However, in these instances the strain gage indicating the greatest strain was checked at small increments of pressure when the ring was near collapse. The pressure was not increased further until the strain gage reading steadied. In the authors' opinion the point of collapse was accurate to - 5 psi. for the very non-circular rings. On the otherhand, failure of the more circular rings occurred rather quickly. During the latter portion of a test run it was customary to pause momentarily at each 5 psi. increment of pressure. Again the authors estimate that the point of collapse was accurate to - 5 psi.

Considering both the accuracy of the pressure reading and the point of failure, the recorded collapse pressure is believed to be within - 10-1/2 psi. or + 5-1/2 psi. of true.

The accuracy of the strain gages used, as stipulated by the manufacturer, was ± 2%. The transverse sensitivity correction was insignificant, being of the order of - 0.05%. An accuracy of one half the smallest scale division on the strain indicator, ± 5 micro-inches per inch , is generally assigned to the switchbox-indicator combination.

As a practical expedient plots of out-of-roundness which are presented in the RESULTS were derived in the following manner; the average diameter was subtracted from the measured diameter at stations and half stations; the difference was divided by two and plotted at diametrically opposite stations. It is to be appreciated that this method will define a symmetrical out-of-roundness curve but is truly representative of the initial configuration only when a symmetrical two lobe pattern predominates.

Correlation of Data

The experimental data is compared to theoretical predictions based upon the following formula:

$$\sigma = \frac{P R}{h} - \frac{6 P R u_o \cos 2\theta}{h^2 (1 - P/P_{crit.})} \qquad (1)$$

Equation (1) was developed for the case of circular tubes in reference (4) but applies equally well to rings; the

Considering both the accuracy of the pressure reading and the point of failure, the recorded collapse pressure is believed to be within - 10-1/2 psi. or + 3-1/2 psi. of true.

The accuracy of the strain gages used, as stipulated by the manufacturer, was ± 2%. The transverse sensitivity correction was insignificant, being of the order of - 0.05%. An accuracy of one half the smallest scale division on the strain indicator, ± 5 micro-inches per inch, is normally assigned to the switchbox-indicator combination.

As a practical expedient plots of out-of-roundness which are presented in the RESULTS were derived in the following manner; the average diameter was subtracted from the measured diameter at stations and half stations; the difference was divided by two and plotted at diametrically opposite stations. It is to be appreciated that this method will define a symmetrical out-of-roundness curve but is only representative of the initial configuration only when a symmetrical two lobe pattern predominates.

Correlation of Data

The experimental data is compared to theoretical predictions based upon the following formula:

$$\epsilon = \frac{p}{E} - \frac{6\ p\ R\ n^2}{E\ t^2\ (1 - p/p_{crit.})} \cos 2\theta \qquad (1)$$

Equation (1) was developed for the case of circular tubes in reference (4) but applies equally well to rings; the

assumptions made in the derivation may be found in the same reference. The major qualifications are that the ring be thin and that the initial configuration be given by $(R + u_o \cos 2\theta)$.

For purposes of computation the authors found it convenient to rearrange and modify equation (1)

$$\sigma = \frac{PR_o}{h} + \frac{6\ P\ Ru_o\ h\ E \cos 2\theta}{Eh^3 - 4PR^3} \qquad (2)$$

$$\varepsilon = \frac{PR_o}{Eh} + \frac{6\ P\ Ru_o\ h \cos 2\theta}{Eh^3 - 4PR^3} \qquad (3)$$

Equation (2) was derived directly from equation (1) by the substitution of $3\ Eh^3/12$ for $P_{crit.}$, R_o for R, and rearranging. Equation (3) is obtained by dividing equation (2) by E. The use of the outside radius, R_o, instead of the radius to the neutral axis, R, in the hoop stress term seemed well taken but changed the predicted strains an insignificant amount.

A common criteria for failure is yielding of the outer fibers due to the addition of hoop stress and the maximum bending stress. Then as a basis for comparison of experimental and theoretical collapse pressures in those cases where the out-of-roundness pattern is $u_o \cos 2\theta$, equation (2) can be reduced to

$$\sigma_{max.} = \frac{PR_o}{h} + \frac{6\ PR\ u_o\ h\ E}{Eh^3 - 4PR^3} \qquad (4)$$

assumptions made in the derivation may be found. If the same reference. The major qualifications are that the ring be thin and that the initial configuration be given by $(R + w_o \cos 2\theta)$.

For purposes of computation the authors found it convenient to rearrange and modify equation (1)

$$\frac{\sigma}{E} = \frac{h}{R_o} + \frac{6\,(1-\nu^2)\,w_o\,h\,R\cos 2\theta}{Eh^3 - 4(1-\nu^2)R^3} \qquad (2)$$

$$\varepsilon = \frac{hw}{R_o^2} + \frac{6\,\rho\,(1-\nu^2)\,w_o\,h\cos 2\theta}{Eh^3 - 4(1-\nu^2)R^3} \qquad (3)$$

Equation (2) was derived directly from equation (1) by the substitution of $3\,w_o^2/12$ for $I^{orit.}$, R_o for R, and rearranging. Equation (3) is obtained by dividing equation (2) by E. The use of the outside radius, R_o, instead of the radius to the neutral axis, R, in the hoop stress term seemed well taken but changed the predicted stress an insignificant amount.

A common criteria for failure is yielding of the outer fibers due to the addition of hoop stress and the maximum bending stress. Then as a basis for comparison of experimental and theoretical collapse pressures in these curved

where the out-of-roundness quotient $= w_o \cos 2\theta$ equation (2) can be reduced to

$$\sigma_{max.} = \frac{h}{R_o} + \frac{6\,(1-\nu^2)\,w_o\,h\,E}{Eh^3 - 4(1-\nu^2)R^3} \qquad (4)$$

When $\sigma_{max.}$ is assumed to be equal to σ_y, the pressure as determined by equation (4) is then the theoretical collapse pressure.

When $\sigma_{max.}$ is assumed to be equal to σ_y, the pressure as determined by equation (4) is then the theoretical collapse pressure.

III

RESULTS

All results presented in this section were derived from data obtained by the authors.

Figure III is a plot of the data obtained during the compression tests of the aluminum alloy specimens and from which the value of Young's Modulus and the yield stress were determined.

Figure IV shows the results of the preliminary test which was made to determine the effect of various lubricants and gaskets upon strain. Lubricant #1 was black rubber-to-metal cement; lubricant #2 was clear rubber cement. Gasket #1 had been used during the Proof Testing; Gasket #2 was of the same dimensions but had not been used previously.

Figures V, VIII, XI, XIV, and XVII show measured and theoretical circumferential strain distributions for one or more pressures. Theoretical curves are based upon equation (3).

Figures VI, IX, XII, XV, and XVIII are plots of out-of-roundness versus circumferential positions.

Figures VII, X, XIII, XVI, and XIX are plots of ring thickness versus circumferential position.

Figures XX-XXVI are a comparison of measured and predicted strains. The experimental points are an average of

III

RESULTS

strains read at the 0° and 180° positions, and 90° and 270° positions. The theoretical curves are based upon equation (3).

Figure XXVII shows experimental collapse points plotted on arguments of pressure and the ratio of out-of-roundness to average thickness.

Figure XXVIII is a comparison of experimental collapse pressures with several theoretical predictions. All theoretical curves are based upon equation (4). They differ in that Curve A is plotted for $\sigma_{max} = \sigma_{y} = 35{,}000$ psi. and $h = h_{ave} = 0.250"$; Curve B is plotted for $\sigma_{max} = 41{,}000$ psi. and $h = h_{ave.} = 0.250"$; Curve C is plotted for $\sigma_{max} = 41{,}000$ psi. and $h = h_{min.} = 0.243"$.

plotted for q_{max} = 41,000 psi. and $h = h_{max.} = 0.243"$.
q_{max} = 41,000 psi. and $h = h_{ave.} = 0.250"$; Curve C is
and $h = h_{ave} = 0.250"$; Curve B is plotted for
in that Curve A is plotted for $q_{max} = q_{\gamma} = 35{,}000$ psi.
theoretical curves are based upon equation (4). They differ
pressures with several theoretical predictions. All
Figure XXVIII is a comparison of experimental collapse
to average thickness.

on arguments of pressure and the ratio of out-of-roundness

Figure XXVII shows experimental collapse points plotted

equation (3).

270^{o} positions. The theoretical curves are based upon

strains read at the 0^{o} and 180^{o} positions. The 90^{o} and

FIGURE III

STRESS STRAIN CURVE

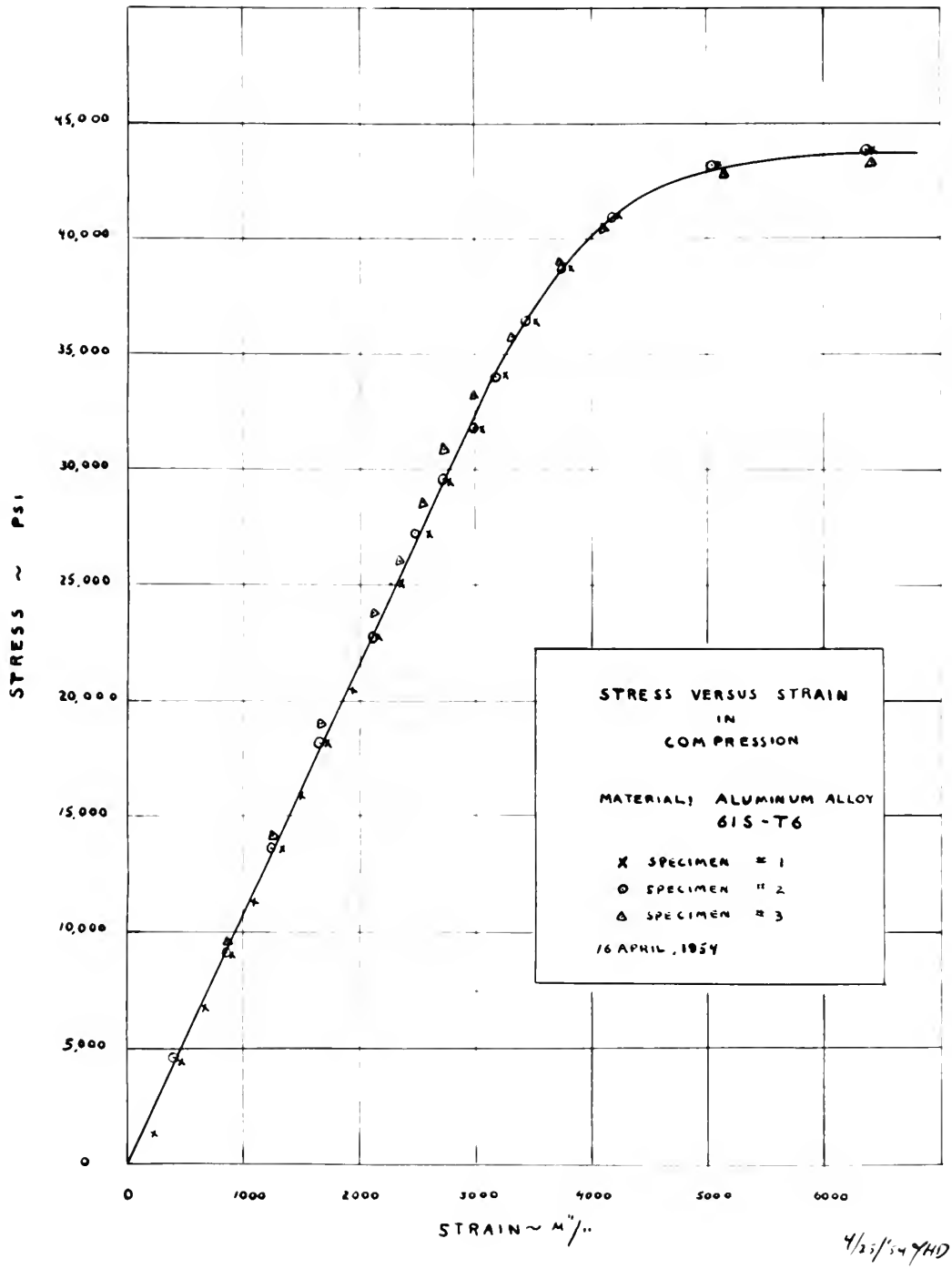

4/23/54 YHD

Figure IV

CIRCUMFERENTIAL STRAIN DISTRIBUTION FOR DIFFERENT LUBRICANTS AND GASKETS
RING NO.-PRELIMINARY TEST

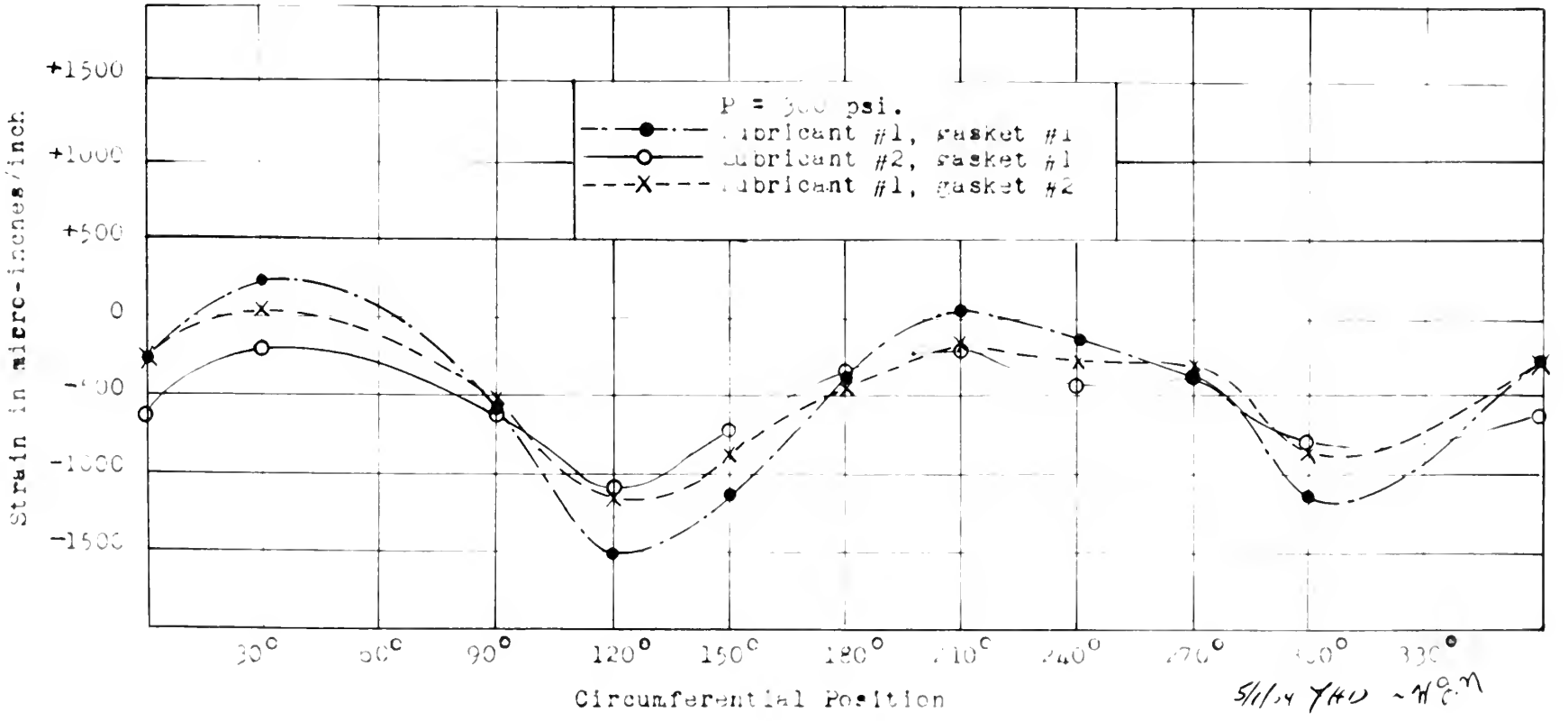

Figure V

CIRCUMFERENTIAL STRAIN DISTRIBUTION ON INNER SURFACE
RING NO. 2 u_o = 0.0118"

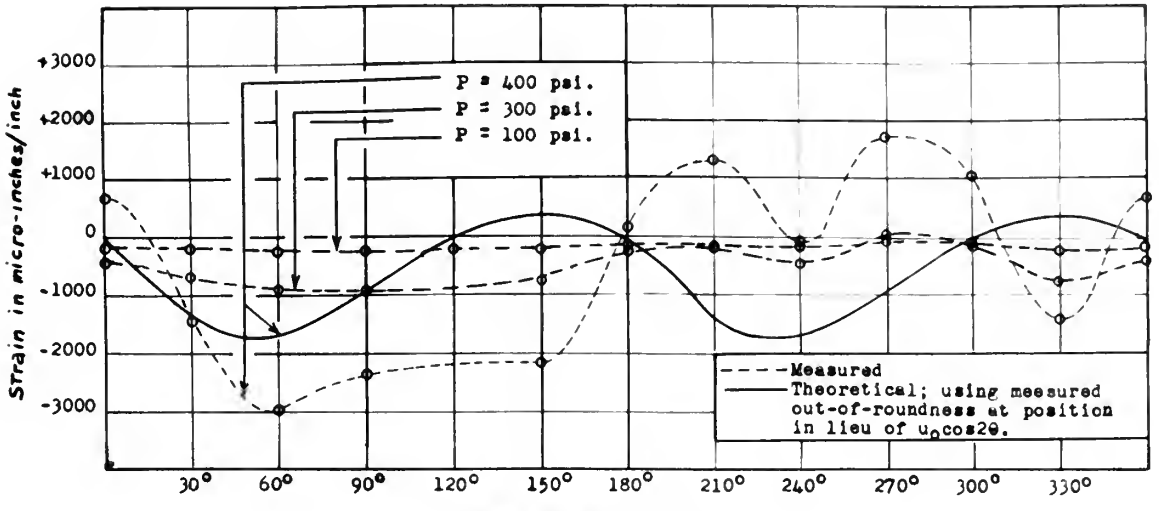

Figure VI

INITIAL CONFIGURATION
RING NO. 2

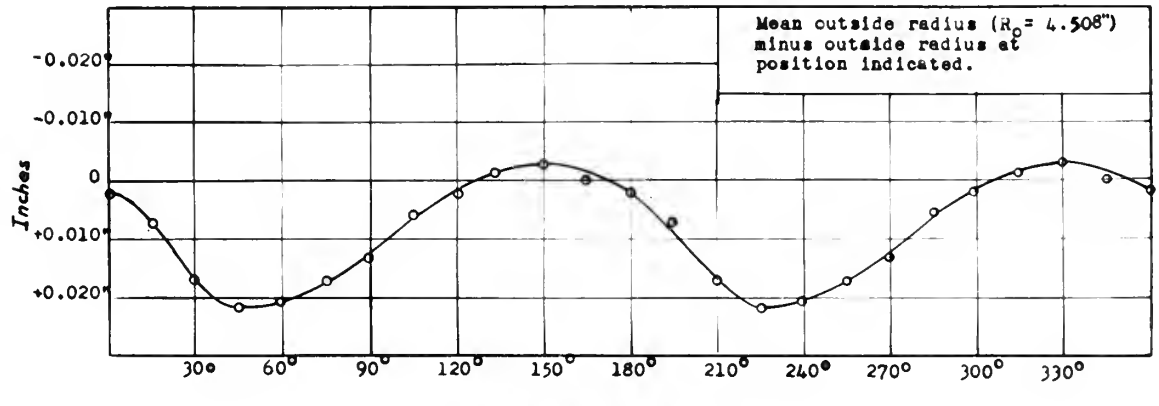

Figure VII

VARIATION IN THICKNESS
RING NO, 2

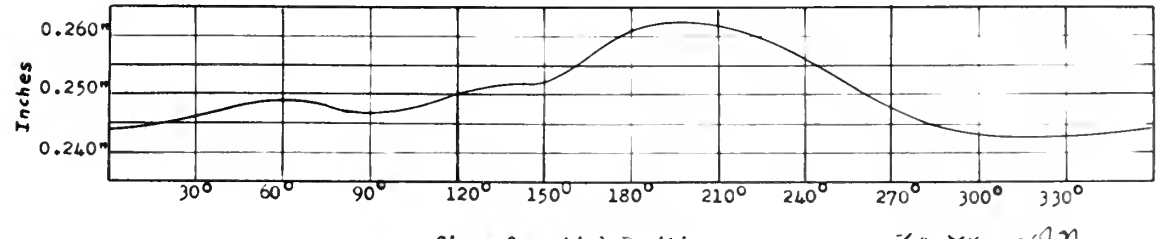

Figure VIII

CIRCUMFERENTIAL STRAIN DISTRIBUTION ON INNER SURFACE
RING NO. 3 u_o = 0.0268"

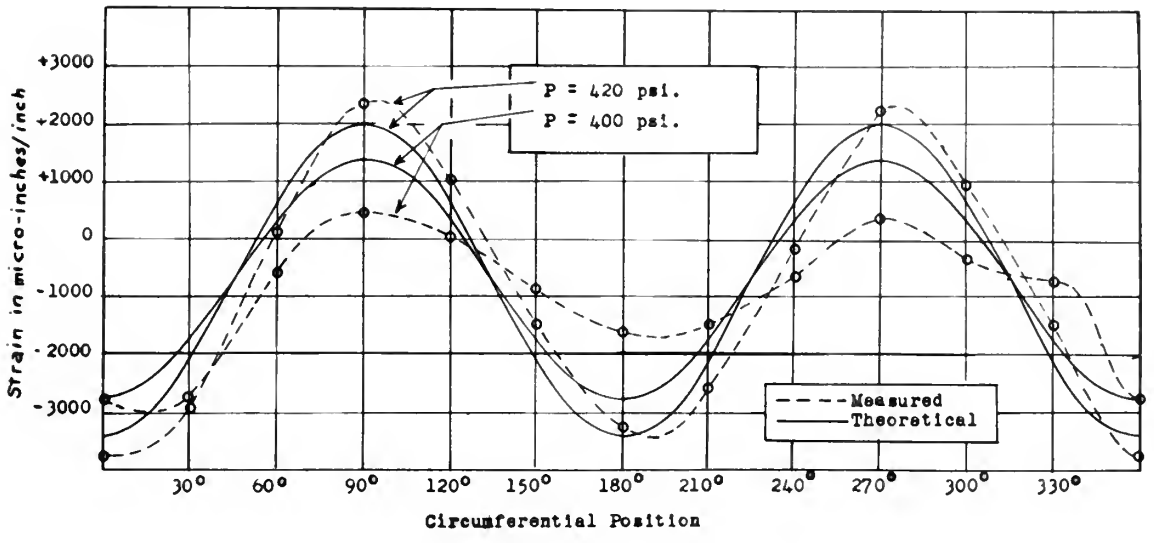

Figure IX

INITIAL CONFIGURATION
RING NO. 3

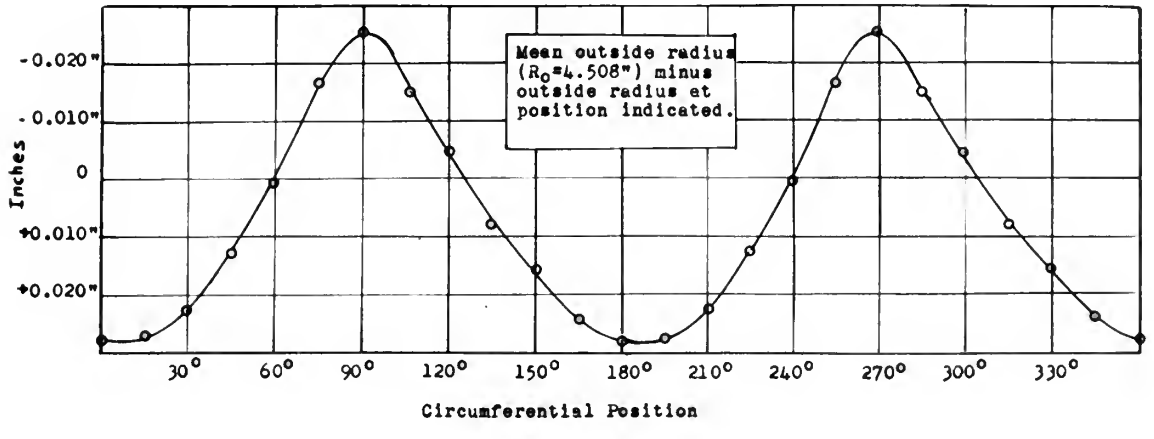

Figure X

VARIATION IN THICKNESS
RING NO. 3

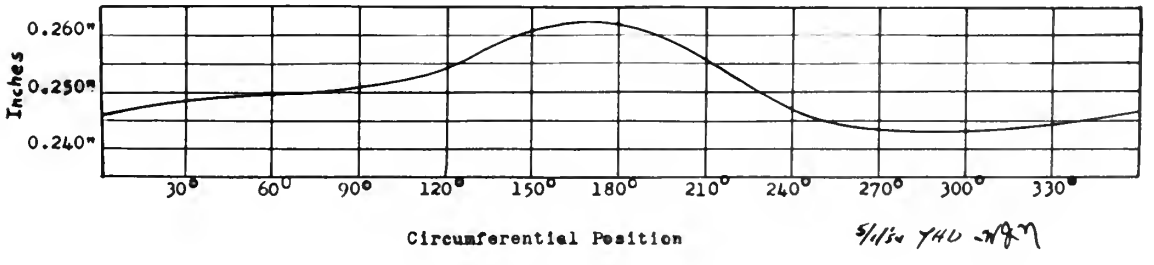

Figure XI

CIRCUMFERENTIAL STRAIN DISTRIBUTION ON INNER SURFACE
RING NO. 5 u_o = 0.0705"

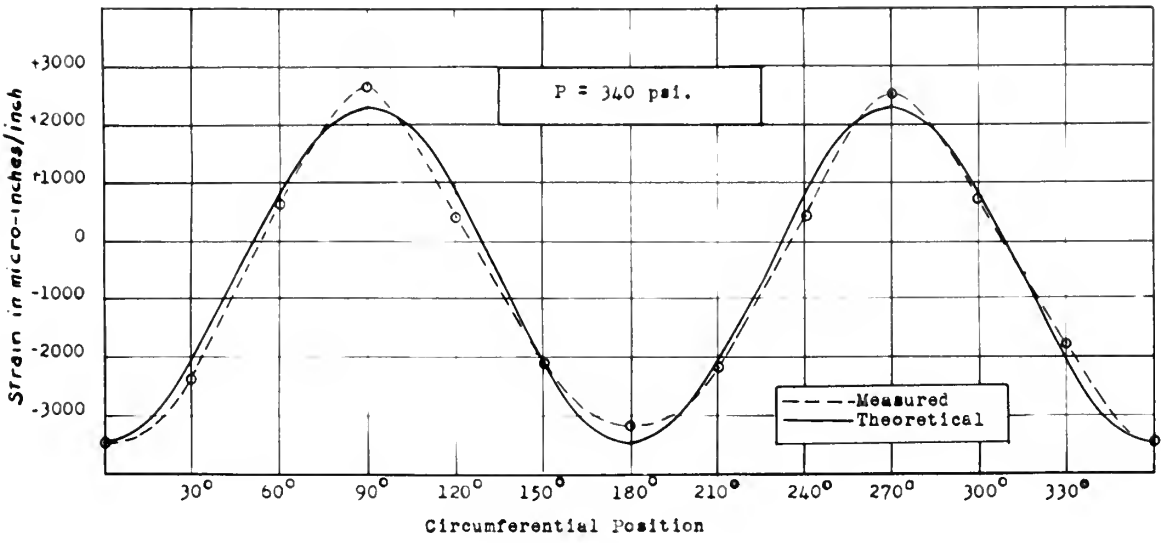

Figure XII

INITIAL CONFIGURATION
RING NO. 5

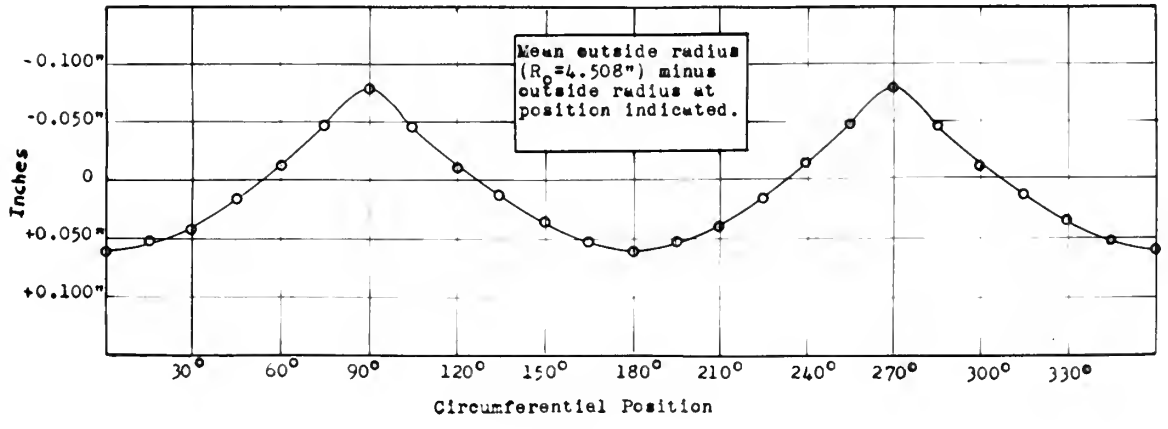

Figure XIII

VARIATION IN THICKNESS
RING NO. 5

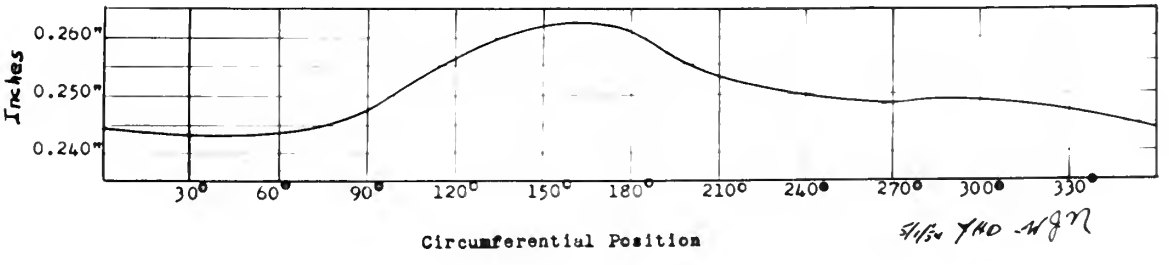

5/1/54 YHO WJM

Figure XIV

CIRCUMFERENTIAL STRAIN DISTRIBUTION ON INNER SURFACE
RING NO. 6 u_o = 0.075"

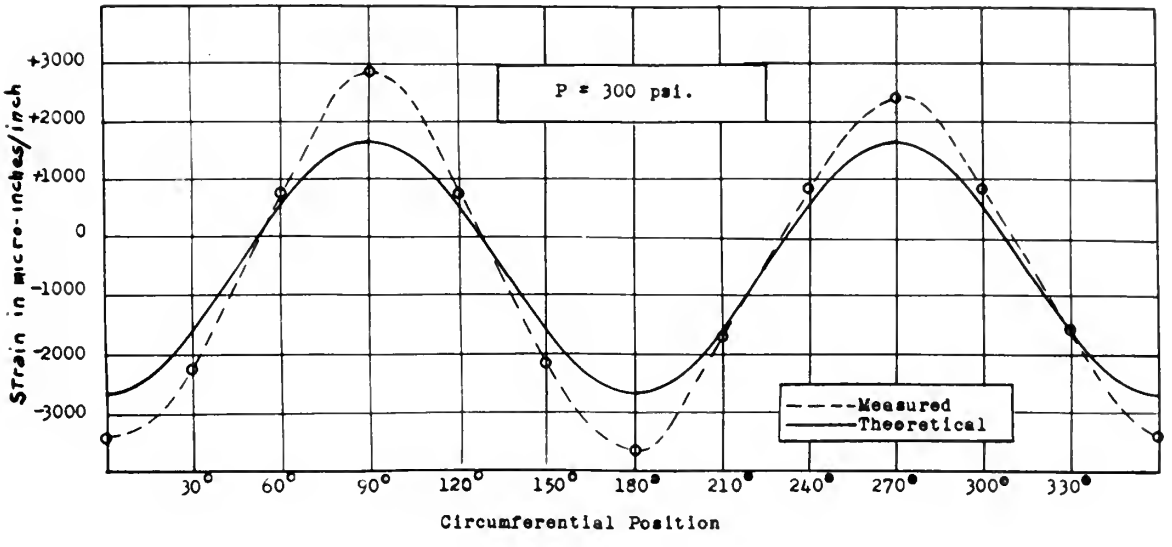

Figure XV

INITIAL CONFIGURATION
RING NO. 6

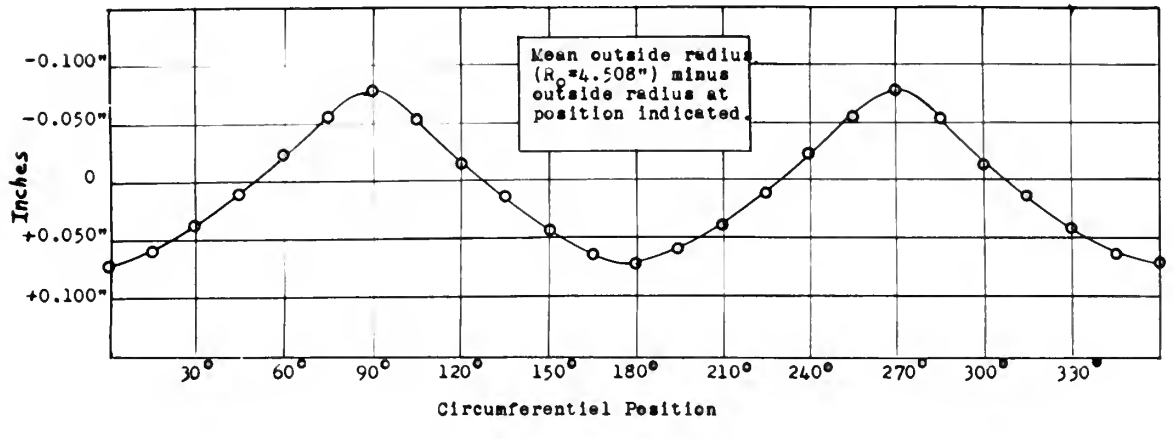

Figure XVI

VARIATION IN THICKNESS
RING NO. 6

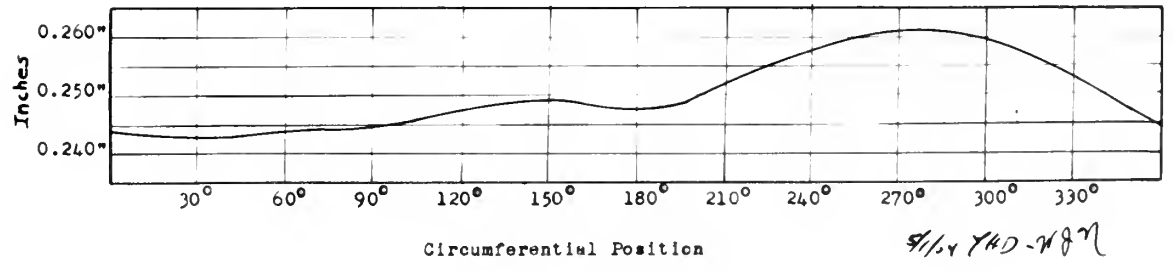

Figure XVII

CIRCUMFERENTIAL STRAIN DISTRIBUTION ON INNER SURFACE
RING NO. 7 u_o = 0.1535"

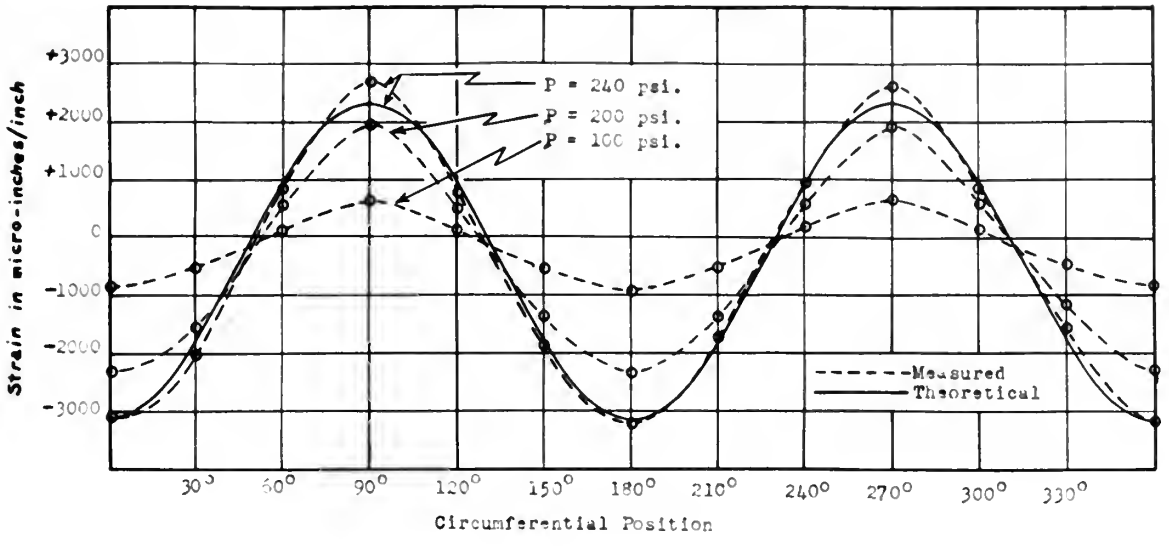

Figure XVIII

INITIAL CONFIGURATION
RING NO. 7

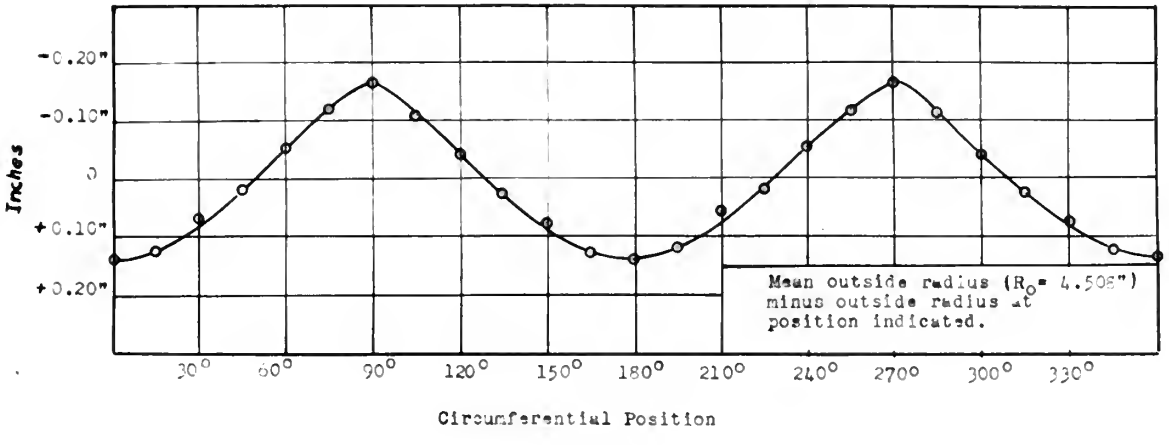

Figure XIX

VARIATION IN THICKNESS
RING NO. 7

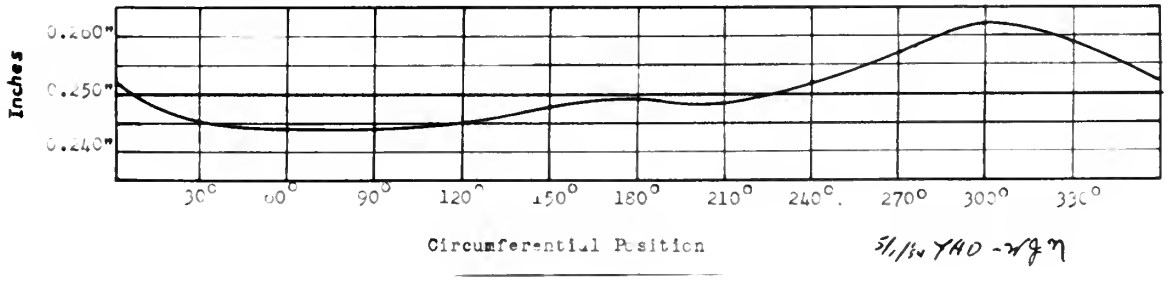

Figure XX

COMPARISON OF MEASURED AND THEORETICAL STRAINS
RING NO. 3 u_o = 0.027"

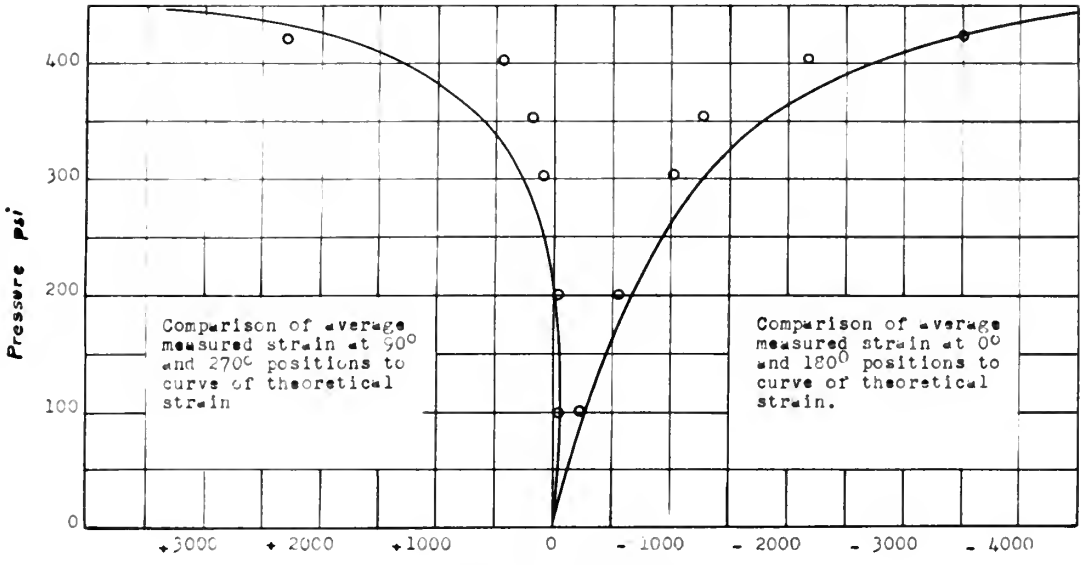

Strain in micro-inches per inch

Figure XXI

COMPARISON OF MEASURED AND THEORETICAL STRAINS
RING NO. 4 u_o = 0.048"

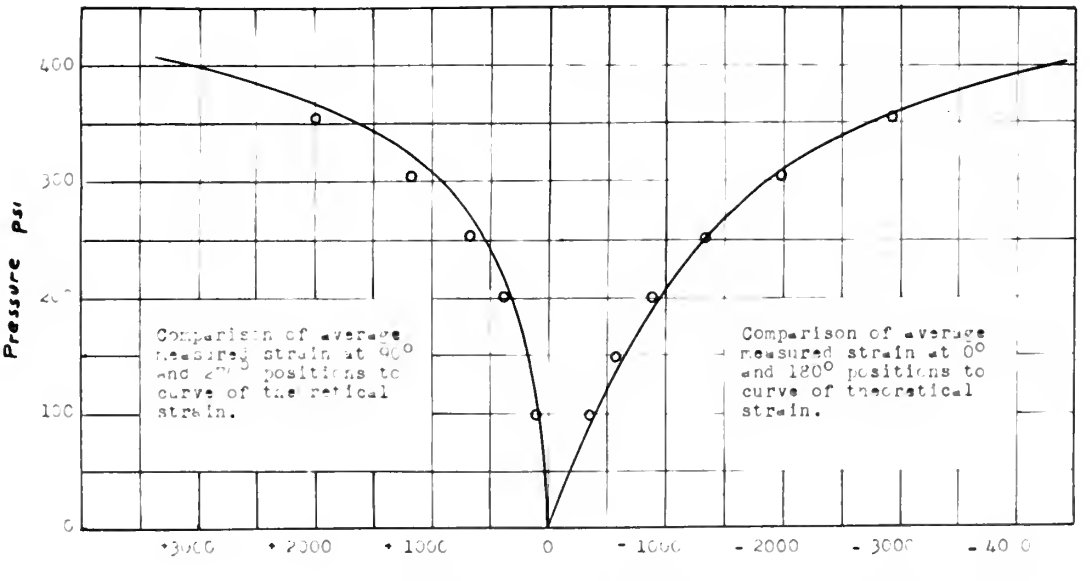

Strain in micro-inches per inch

5/15/54 RAD-RGR

Figure XXII

COMPARISON OF MEASURED AND THEORETICAL STRAINS
RING NO. 5 u_o = 0.070"

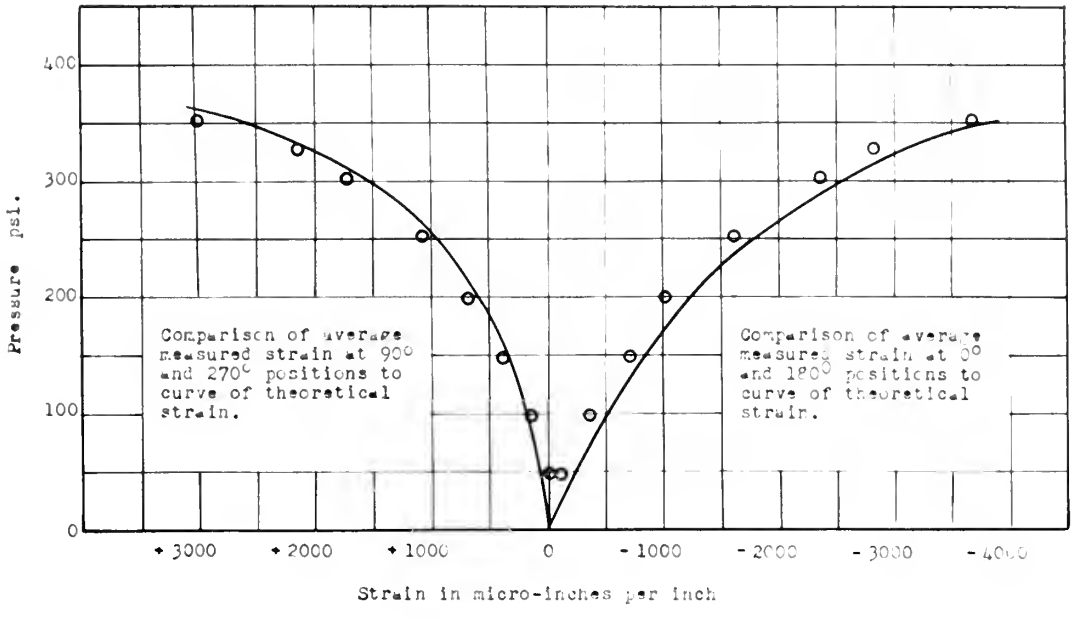

Figure XXIII

COMPARISON OF MEASURED AND THEORETICAL STRAINS
RING NO. 6 u_o = 0.075"

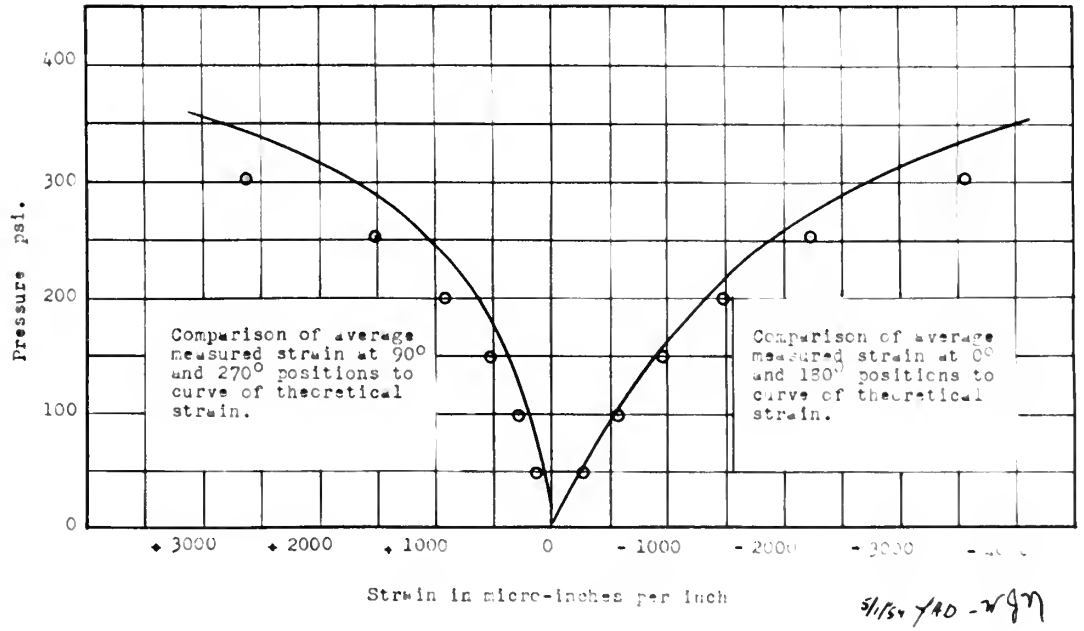

Figure XXIV

COMPARISON OF MEASURED AND THEORETICAL STRAINS
RING NO. 7 u_o = 0.1935"

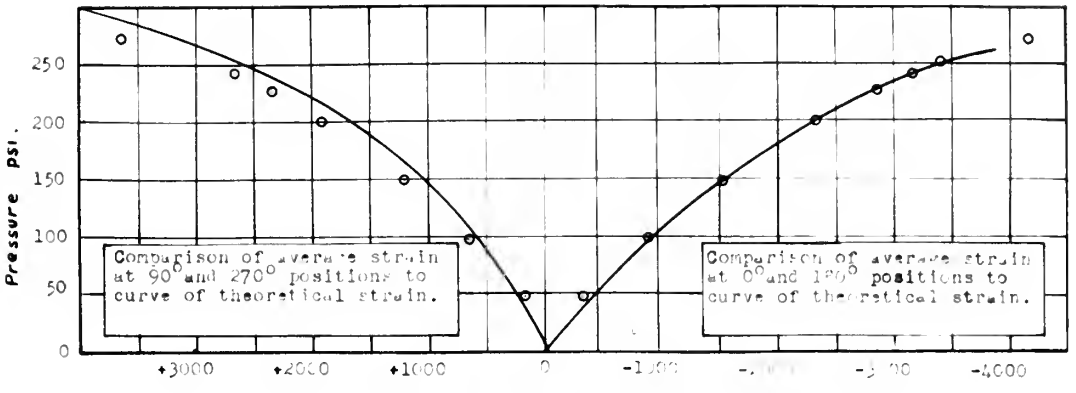

Figure XXV

COMPARISON OF MEASURED AND THEORETICAL STRAINS
RING NO. 8 u_o = 0.204"

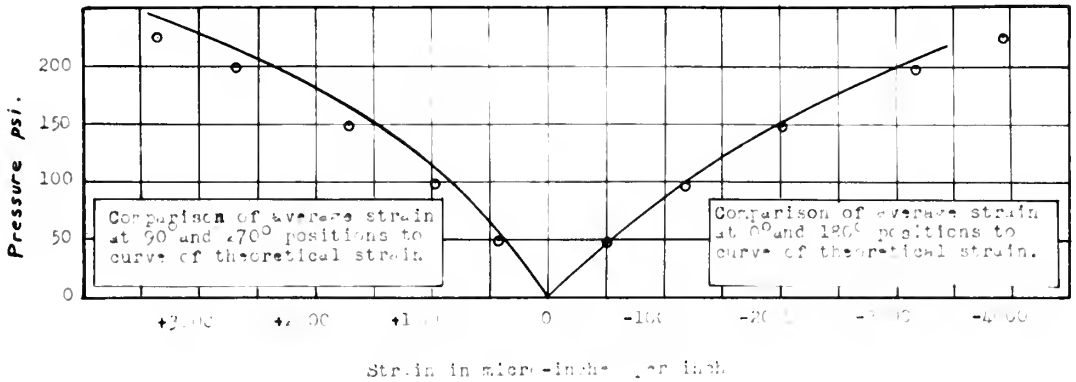

Figure XXVI

COMPARISON OF MEASURED AND THEORETICAL STRAINS
RING NO. 9 u_o = 0.203"

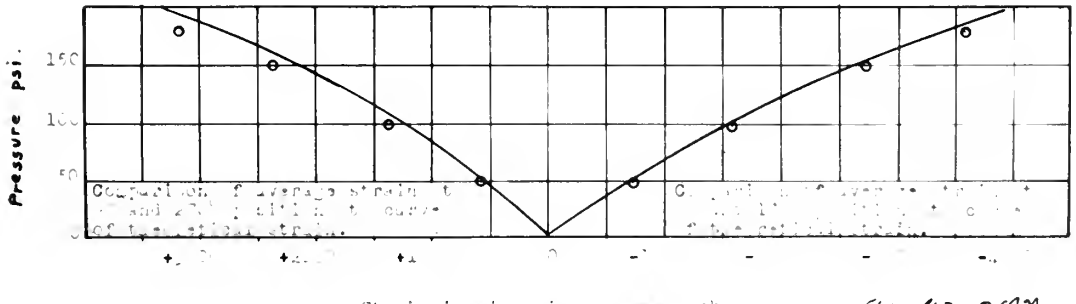

5/15/54 AD - 2497

Figure XXVII

COMPARISON OF MEASURED AND PREDICTED BUCKLING PRESSURES

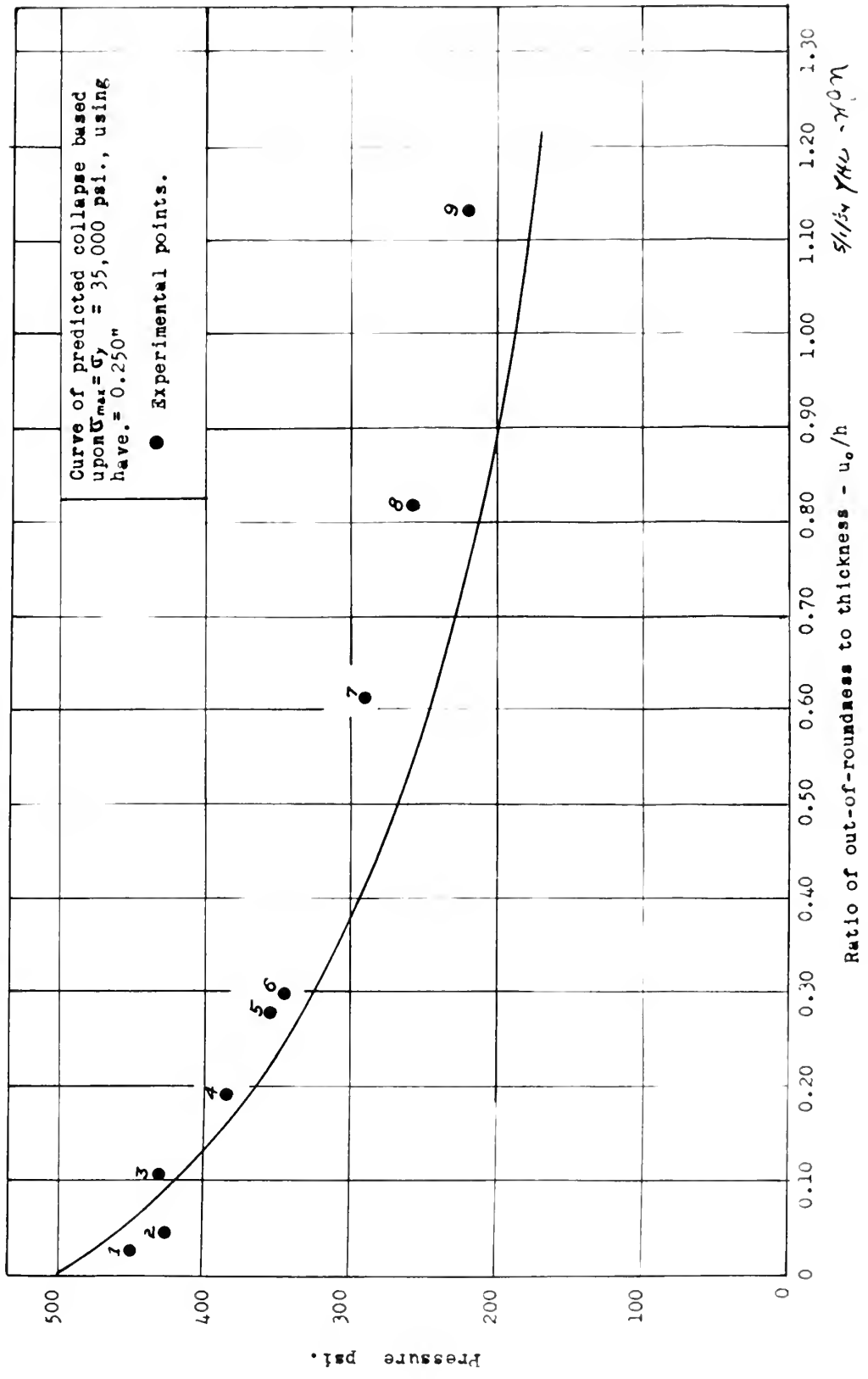

Figure XXVIII

COMPARISON OF MEASURED AND PREDICTED BUCKLING PRESSURES

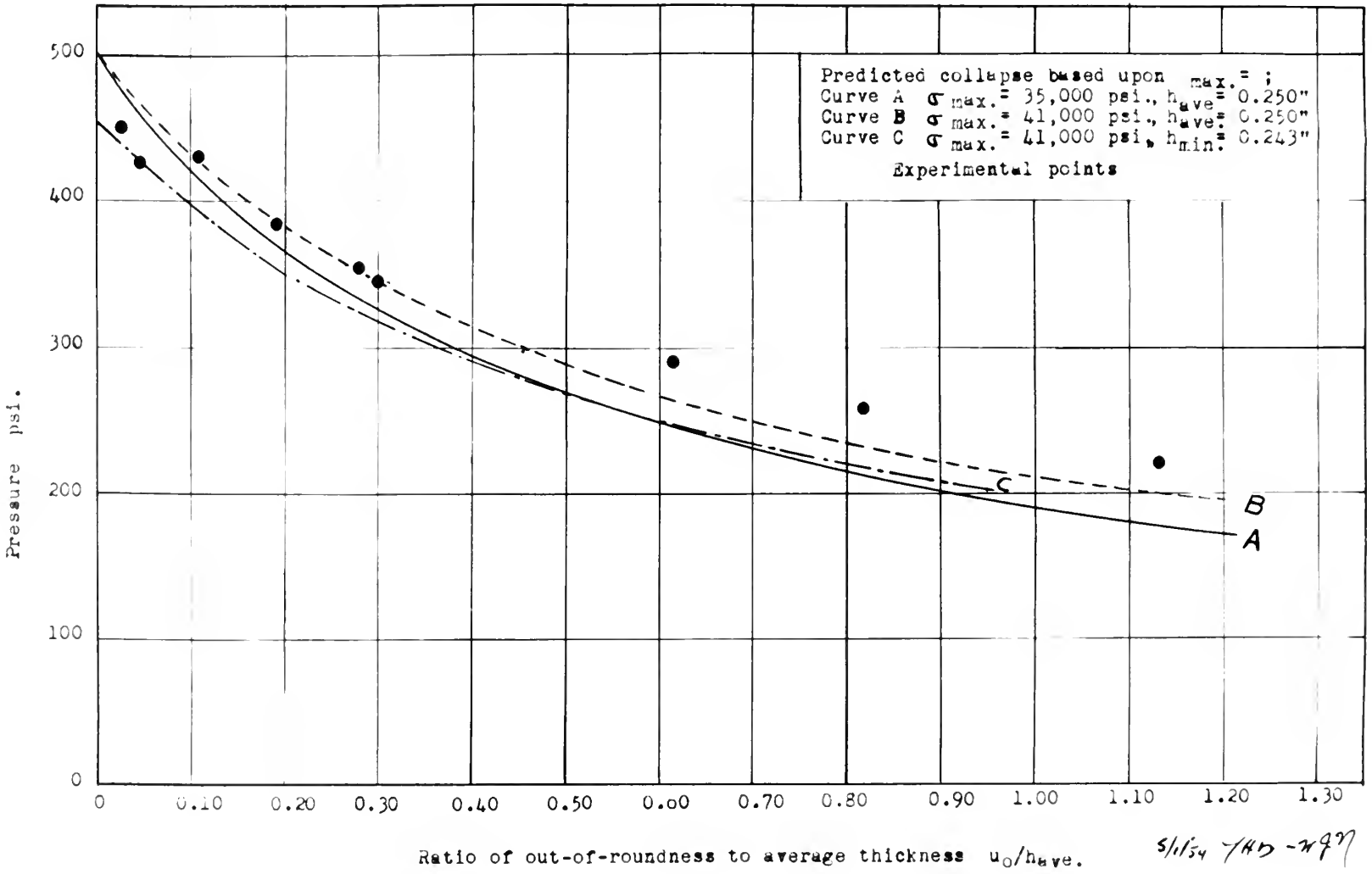

5/1/54 YHD -mgg

IV.

DISCUSSION OF RESULTS

Introduction

For convenience and continuity, the experimental results may be grouped in the following sequence:

1. Results of Compression Tests
2. Proof Test Data
3. Circumferential Strain Distributions
4. Maximum Strains
5. Collapse Pressures

This classification is convenient in that the significance of any group depends to some extent upon the interpretation and validity attached to one or more of the preceding groups.

Results of Compression Tests

The results obtained from the compression tests were probably the most significant factors in the correlation of experimental and theoretically predicted quantities.

The data obtained from the tests of the specimens were surprisingly consistent. See Figure III. Values of strain correlate particularly well at high stresses where some deviation might be expected. The possibility of introducing rather significant errors during the resetting of the Huggenberger Tensometers was considered,

IV.

DISCUSSION OF RESULTS

Introduction

For convenience and continuity, the experimental results may be grouped in the following sequence:

1. Results of Compression Tests
2. Proof Test Data
3. Circumferential Strain Distributions
4. Maximum Strains
5. Collapse Pressures

This classification is convenient in that the significance of any group depends to some extent upon the interpretation and validity attached to one or more of the preceding groups.

Results of Compression Tests

The results obtained from the compression tests were probably the most significant factors in the correlation of experimental and theoretically predicted quantities.

The data obtained from the tests of the specimens were surprisingly consistent. See Figure III. Values of strain corresponding reasonably well within the
where some deviation [illegible]
or introduced. [illegible]
results of the [illegible]

but a review of the data indicated that increments of strain before and subsequent to a reset were consistent. That the stress-strain curve shown in Figure III is representative of the alloy from which the rings were manufactured is implied in preceding sections. Appreciating the fact that the proof stress and ultimate strength of aluminum alloy varies considerably with the details of the heat treatment and possibly the original lot number, the authors specified that the specimens be obtained from the length of tubing from which the rings were manufactured and that all rings and specimens be heat treated as a group.

Young's Modulus, as determined from the stress-strain curve, was 10.8×10^6 psi. and can be compared to $E = 10 \times 10^6$ psi., the value generally given in handbooks. In the authors' opinion, Figure III justified the assumption of a linear stress-strain relationship up to a stress of 34,500 psi. and a 0.2% proof stress, designated yield stress, of 35,000 psi. Furthermore, it is to be noted that a very distinct departure from linearity did not occur until a stress of about 41,000 psi. was obtained.

These properties were commensurate with those characteristics considered most desirable in the material from which the rings were made. The existence of a linear stress-strain relationship over a large range of stress

permitted most of the experimental strains to be compared directly with predictions based upon equation (3) without the complication of a decreasing modulus. For extrapolation of the results to steel rings, a plateau corresponding to a true yield stress was desirable. Although the authors did not anticipate such similarity at the time aluminum alloy was selected, the upper portion of the stress-strain curve is in most respects analogous to the compression test curves obtained for mild steel specimens tested by M. L. Pittman, Jr., and V. W. Rinehart (7).

It may be argued that the remainder of the results would have been of no consequence without the stress-strain data. The use of a standard stress-strain curve for aluminum alloy 61S-T6 would have involved an 8% error in Young's Modulus and a 14% error in the proof stress. Furthermore, the shape of the curve above the proof stress is valuable when analyzing the failure of a ring.

Proof Test Data

The authors have stated that the measured strains at a specified pressure were dependent to some extent upon the gasket and the type of lubricant used between the gasket and the Plexiglas surfaces. Figure IV shows this effect quantitatively. Black rubber-to-metal cement has been designated Lubricant #1 and clear rubber cement as

permitted most of the experimental strains to be compared directly with predictions based upon equation (3) without the complication of a decreasing modulus. For extrapolation of the results to steel rings, a plateau corresponding to a true yield stress was desirable. Although the authors did not anticipate such similarity at the time aluminum alloy was selected, the upper portion of the stress-strain curve is in most respects analogous to the compression test curves obtained for mild steel specimens tested by M. L. Hitman, Jr., and W. M. Rinehart (7).

It may be argued that the remainder of the results would have been of no consequence without the stress-strain data. The use of a standard stress-strain curve for aluminum alloy 618-T6 would have involved an 8% error in Young's Modulus and a 14% error in the proof stress. Furthermore, the shape of the curve above the proof stress is valuable when analyzing the failure of a ring.

Proof Test Data

The authors have stated that the measured strains at a specified pressure were dependent to some extent upon the gasket and the type of lubricant used between the gasket and the flexrigs surfaces. Figure IV shows this effect quantitatively. Black rubber-to-metal contact was

Lubricant #2. Although Lubricant #1 was considered most suitable on the basis of a preliminary investigation which has been described, Lubricant #2 appeared to be a reasonable second choice. The two gaskets were of the same dimensions and material but differed in that Gasket #1 had been used several times before while Gasket #2 had not. Relative to Gasket #2, Gasket #1 was very limber and appeared to have a slick, oily surface.

As shown by Figure IV the largest measured strains were attained with Lubricant #1 and Gasket #1. Lubricant #1, Gasket #2 were next in magnitude of strains while Lubricant #2, Gasket #1 gave the smallest measured strains. Considered as percentages, the differences in strains are quite significant. The authors reasoned that the gasket and lubricant were able to affect the strains by changing the magnitude of the friction force acting at the gasket-Plexiglas interface.

On the basis of the results indicated by Figure IV, the authors elected to use a well broken-in gasket in conjunction with Lubricant #1 for the remainder of the tests since this combination more nearly satisfied the requirement that the ring be completely free of restraint at the edges.

A thorough investigation of the friction force at the

Lubricant #2. Although lubricant #1 was considered most suitable on the basis of a preliminary investigation which has been described, lubricant #2 appeared to be a reasonable second choice. The two gaskets were of the same dimensions and material but differed in that gasket #1 had been used several times before while Gasket #2 had not. Relative to Gasket #2, Gasket #1 was very limber and appeared to have a slick, oily surface.

As shown by Figure IV the largest measured strains were attained with Lubricant #1 and Gasket #1. Lubricant #1, Gasket #2 were next in magnitude of strains while Lubricant #2, Gasket #1 gave the smallest measured strains. Considered as percentages, the differences in strains are quite significant. The authors reasoned that the gasket and lubricant were able to effect the strains by changing the magnitude of the friction force acting at the gasket-Plexiglas interface.

On the basis of the results indicated by Figure IV, the authors elected to use a well broken-in gasket in conjunction with lubricant #1 for the remainder of the tests since this combination more nearly satisfied the requirements that the ring be completely free or restraint at its edges.

A thorough investigation of the friction force in the

gasket-Plexiglas interface should be a prerequisite for further experimentation based upon this thesis. The objectives of such an investigation should be a consideration of all likely gaskets and lubricants, a comparison of possible combinations with respect to effect upon strains, and a quantitative evaluation of the coefficient of friction characteristic of given combinations of gasket, lubricant and pressure.

Circumferential Strain Distribution

Figures VI, IX, XII, XV, and XVIII show typical out-of-roundness curves. Of the rings shown in this group, all were deformed intentionally with the exception of Ring No. 2, Figure VI. It is significant that the out-of-roundness obtained in Ring No. 2, while purely arbitrary, is very similar to a configuration given by $u_o \cos 2\theta$. The remainder of the plots are characterized by rather steep peaks in the vicinity of the minimum diameter and shallow peaks at points of maximum diameter. It is to be noted that the steep peaks occurred at points where the deforming loads were applied by the loading machine. The configurations are, however, reasonably similar to a cosine curve of the form $u_o \cos 2\theta$.

Figures VII, X, XIII, XVI, and XIX show the variation in thickness versus circumferential position. It is apparent that the relation of thickness and out-of-roundness at a

gasket-flexible rubberes should be a preferable for further experimentation based upon this theory. The objectives of such an investigation should be a consideration of all likely gasket and lubricants, a comparison of possible combinations with respect to effect upon strips, and a quantitative evaluation of the coefficient of friction, characteristic of given combinations of gasket, lubricant and pressure.

Circumferential Strain Distribution

Figures VI, IX, III, X, and VIII show typical out-of-roundness curves. Of the rings shown in this group, all were deformed identically with the exception of Ring No. 2, Figure VI. It is significant that the out-of-roundness obtained in Ring No. 2, while purely arbitrary, is very similar to a configuration given by $n\theta$ cos θ. The reciprocity of the plots are characterized by rather steep peaks in the vicinity of the minimum diameter and portion peak at points of maximum diameter. It is to be noted that the strain peaks occurred at points where the eccentric loads were applied by the loading machine. The configurations were, however, reasonably similar to a cosine curve of the form $n\theta$ cos θ.

Figures VII, X, III, etc. show the variation in thickness around circular [illegible]. It is [illegible] that the relation of thickness [illegible]

particular station is completely arbitrary. In general, the difference between minimum and maximum thickness is of the order of 0.02". Since the out-of-round plot is derived from the diameters read to the outer circumference, the corresponding configuration of the neutral axis may be assumed to deviate slightly from that of the plot. Since sections of thickness greater than average were generally opposite sections of less than average, the effect of this deviation upon the measured value of u_o is assumed to be of no consequence except in the circular rings. During a preliminary reduction of data the authors considered the effect which a variation in thickness might have upon the plots of out-of-roundness and predicted strains. The plot of out-of-roundness for Ring No. 2 was altered to a minor extent. The plots for other rings were affected an insignificant amount. Correlation of measured and predicted strains was not improved.

With respect to circumferential strain distributions essentially three types of results were obtained. Figure V shows an arbitrary distribution while Figure XVII shows a well defined cosine distribution. Ring No. 3, Figure VIII, appears to combine some of the characteristics of the first two types.

The arbitrary distribution occurred in those rings

which were essentially circular. The theoretical curve shown in Figure V is a plot of equation (3) with the measured out-of-roundness at a particular position substituted for $u_o \cos 2\theta$ and with $h = h_{ave} = 0.250"$. A point of interest is the fact that the small peaks which are visible at low pressures define a pattern which would seem to persist up to the maximum pressures obtained. The pattern is characterized by a relatively constant strain over 60° or 90° of the circumference and a fluctuating strain over the remaining 300° or 270°; the fluctuations are a reasonable representation of two cycles of a cosine curve. The fact to be observed is that correlation between out-of-roundness and strain distribution is completely lacking.

Subsequent results demonstrate quite clearly that theoretical and measured strains agree satisfactorily when the initial configuration assumed in equation (3) is actually obtained in the ring. It is possible, then, that the method of measuring out-of-roundness was not sufficiently accurate in the case of Ring No. 2. In appraising the out-of-roundness measurement, it is convenient to visualize the initial configuration of the ring as a series of the form $R_o + u_o \cos 2\theta + u_1 \cos 3\theta + u_2 \cos 4\theta - - - u_n \cos (n + 2)\theta$. The measurements from which Figure VI

$N_n \cos(n + 2)\theta$. The measurements from which Figure VI

form $J_0 + J_0 \cos^2\theta + J_1 \cos 2\theta + J_2 \cos$ = - -

the initial configuration of the ring as a series of the

out-of-roundness measurement, it is convenient to visualize

accurate in the case of Ring No. 2. In appraising the

the method of measuring out-of-roundness was not sufficiently

actually obtained in the ring. It is possible, then, that

the initial configuration assumed in equation (3) is

theoretical and measured strains agree satisfactorily when

Subsequent results demonstrate quite clearly that

pletely lacking.

between out-of-roundness and strain distribution is com-

curve. The fact to be observed is that correlation

are a reasonable representation of two cycles of a cosine

strain over the remaining 300^o or 270^o; the fluctuations

over 60^o or 90^o of the circumference and a fluctuating

pattern is characterized by a relatively constant strain

to persist up to the maximum pressures obtained. The

visible at low pressures define a pattern which would seem

of interest is the fact that the small peaks which are

tuted for $N_o \cos 2\theta$ and with $h = h_{ave} = 0.250"$. A point

measured out-of-roundness at a particular position substi-

shown in Figure V is a plot of equation (3) with the

which were essentially circular. The theoretical curve

was obtained reflect only those terms of the form $u_0 \cos 2\theta$, $u_2 \cos 4\theta$, $u_4 \cos 6\theta$, etc. It is to be observed that of these terms $u_0 \cos 2\theta$ appears to predominate. Nevertheless, the assumption of a simple contour, $R_0 + u_0 \cos 2\theta$, in equation (3) may not be justified since the effect of odd terms ($u_1 \cos 3\theta$, $u_3 \cos 5\theta$, etc.) is not indicated by Figure VI. On the other hand, the effect of this omission upon the predicted strain distribution is not so serious as might be expected. If a relation corresponding to equation (3) is derived assuming a configuration such as $R_0 + u_1 \cos 3\theta$, it will be found that the maximum bending stress is proportional to $\frac{1}{1-P/P_{crit}}$ where P_{crit} is the buckling pressure of a circular ring into (n+2) lobes. The buckling pressure, P_{crit}, increases rapidly with the number of lobes; thus the value of P_{crit} for a two-lobe collapse is three-eights of P_{crit} for a three lobe collapse and one-fifth of P_{crit} for a four lobe collapse. Consequently even if u_1, u_2, u_3, etc. are comparable in magnitude to u_0 the effect upon the strain distribution will be considerably less since the bending stress is governed by $\frac{1}{1-P/P_{crit}}$. In view of these facts the arbitrary strain distribution appears to be the result of a rather complicated combination of inadequate measure-

ment, variation of thickness, and localized surface irregularities or dents.

It follows, however, that a more thorough investigation of essentially circular rings is warranted. Rings could be machined as circular as possible and to a close tolerance in thickness. If the initial contour were then determined precisely, it would be possible to evaluate the effect of deviations from a basic two lobe pattern such as that given in Figure VI. It is the authors' opinion that under these circumstances the method of measuring out-of-roundness used in this thesis would prove useful as a practical measure, especially at high pressures.

Ring No. 3 appeared to be the borderline case. With reference to Figure VIII it is apparent that the circumferential strain distribution at 400 psi. deviated considerably from the theoretical curve, equation (3) with $h = h_{ave} = 0.250"$. The distribution is not a clearly defined cosine curve, and the magnitude of the strains are generally below the predicted values. On the other hand, at 420 psi. there was a visible deflection of the ring and the strain distribution assumed a form which, except for a 4^{o}-8^{o} phase shift, compared favorably with predicted values. At 400 psi. the deviations from a pure cosine curve are of the same character as the superposition of harmonics upon

ment, variation of thickness, and localized curious irregularities or dents.

It follows, however, that a more thorough investigation of essentially circular rings is warranted. Rings could be machined as circular as possible and to a close tolerance in thickness. If the initial contour were then determined precisely, it would be possible to evaluate the effect of deviations from a basic two lobe pattern such as that given in Figure VI. It is the authors' opinion that under these circumstances the method of measuring out-of-roundness used in this thesis would prove useful as a practical measure, especially at high pressures.

Ring No. 3 appeared to be the borderline case. With reference to Figure VIII it is apparent that the circumferential strain distribution at 400 psi. deviated considerably from the theoretical curve, equation (3) with $n = \text{have} = 0.250$". The distribution is not a cleanly defined cosine curve, and the magnitude of the strains are generally below the predicted values. On the other hand, at 450 psi. there was a visible deflection of the ring and the strain distribution assumed a [illegible]. Except for a 4°-8° phase shift, compared favorably [illegible] at 400 psi. The deviations from a pure cosine curve are of the same character as the superposition of harmonics upon

a fundamental wave form. Here it is possible to reason that the terms $u_1 \cos 3\theta$, $u_2 \cos 4\theta$, etc. are significant relative to the basic two lobe pattern given by $R_o + u_o \cos 2\theta$. At 420 psi a two lobe strain pattern was clearly predominate; this would be expected since as the pressure approaches P_{crit} for the two lobe collapse pattern, the bending strains become significantly greater than corresponding strains resulting from the superposition of other basic configurations. However, in view of the added complication of the thickness variation and possible localized irregularities the authors do not feel justified in attributing the entire cause of the deviations to an inadequate out-of-round measurement. Again it is suggested that the effect of any deviation from a basic two lobe out-of-round pattern requires further investigation.

The last type of strain distribution, the clearly defined cosine curve, is exemplified by Rings No. 5 and 7, Figures XI-XIII and XVII-XIX. With the exception of Ring No. 6, the plots are typical of the results and correlation observed in Rings No. 4-9. Despite the peaked out-of-roundness curve and the variation in thickness, the correlation of measured and predicted strains is excellent. The manner in which the initial peaks of the strain curve progressively increase in amplitude is clearly demonstrated in Figure XVII. Any deviations from the basic two

ted in Figure XVII. Any deviations from the [illegible]

progressively increase in amplitude is clearly demonstra-

ble. The manner in which the initial peaks of the first curve

coincidence or measured and predicted strains is excellent.

of-roundness curve and the variation in thickness, the

lation observed in Rings No. 4-9. Despite the peaked out-

Ring No. 9, the plots are typical of the results and curve-

Figures XI-XIII and XVII-XIX. With the exception of

defined cosine curve, is exemplified by Rings No. 5 and 7,

The last type of strain distribution, the clearly

of-round pattern requires further investigation.

that the effect of any deviation from a basic two lobe out-

investigate out-of-round measurement. Where it is suggested

in attributing the entire cause of the deviation to an

localized irregularities the authors do not feel justified

complication of the thickness variation and possible

other basic configurations. However, in view of the added

responding strains resulting from the superposition of

the bending strains become significantly greater than cor-

pressure spheroides Point for the two lobe collapse pattern,

clearly predominate; this would be expected since as the

$K^0 + K^0 \cos 2\theta$. At 420 psi a two lobe strain pattern was

relative to the basic two lobe pattern given by

that the terms $K^1 \cos 3\theta$, $K2 \cos 4\theta$, etc. are significant

a fundamental wave form. Here it is possible to reason

lobe pattern were insignificant at all pressures.

The test of Ring No. 6 differed from the others in that the Plexiglas surfaces were coated with black rubber-to-metal cement before the ring was placed in the test chamber. The gasket and outer surface of the ring were coated in the usual manner. This deviation from the usual test procedure was made in order to determine whether or not the friction between the gasket and Plexiglas could be reduced still further. The results of this test are shown in Figure XIV. The correlation of measured and predicted strains should be compared with that obtained in Figure XI since Rings No. 5 and 6 were of comparable out-of-roundness, u_o = 0.0705" and u_o = 0.075" respectively. Where excellent correlation was observed for Ring No. 5, the maximum strains in Ring No. 6 were as much as 40% above the predicted values. This discrepancy cannot be explained by the authors. Were it not for the fact that the results of Rings No. 4, 5, 7, 8, and 9 consistently plotted along the predicted strain curves, it might be assumed that in all cases other than Ring No. 6 a significant restraining force was present at the gasket-Plexiglas interface. The fact that such consistency does exist would imply that the test of Ring No. 6 was faulty in some respect. The results definitely indicate a need for further investigation of the friction force at

lobe pattern were insignificant at all pressures.

The test of Ring No. 6 differed from the others in that the Plexiglas surfaces were coated with black rubber-to-metal cement before the ring was placed in the test chamber. The gasket and outer surface of the ring were coated in the usual manner. This deviation from the usual test procedure was made in order to determine whether or not the friction between the gasket and Plexiglas could be reduced still further. The results of this test are shown in Figure XIV. The correlation of measured and predicted strains should be compared with that obtained in Figure XI since Rings No. 5 and 6 were of comparable out-of-roundness, $x_0 = 0.0705"$ and $x_0 = 0.075"$ respectively. Where excellent correlation was observed for Ring No. 5, the maximum strains in Ring No. 6 were as much as 40% above the predicted values. This discrepancy cannot be explained by the authors. Nore it not for the fact that the results of Rings No. 4, 5, 7, 8, and 9 consistently plotted along the predicted strain curves, it might be assumed that in all cases other than Ring No. 6 a significant restraining force was present at the gasket-Plexiglas interface. The fact that such con-sistency does exist would imply that the test of Ring No. 6 was faulty in some respect. The results tentatively indicate a need for further investigation of the friction force at

the gasket-Plexiglas interface, such as suggested previously.

Maximum Strains

In those rings which were intentionally deformed strain gages were placed at points of maximum (0° and 180°) and minimum (90° and 270°) diameters. The strains at 0° and 180° were averaged and plotted for Rings No. 3-9 on the right side of Figures XX - XXVI. Similarly, the average of the 90° and 270° readings are shown on the left side of the same plots. The theoretical curve is simply a plot of equation (3) with cos 2 θ equal to plus or minus one and $h = h_{ave.} = 0.250"$. The strains at 0° and 180° are particularly important in that they are normally used in the prediction of a collapse pressure; consequently, the strains at these positions are given added consideration.

With the exception of Rings No. 3 and 6, the correlation of measured and theoretical strain is entirely satisfactory. On the pressure scale the compressive strains are generally within a range of $\pm$5-1/2 psi. of the theoretical curve; this was the assumed accuracy of the recorded pressure. The tensile strains always appear below the theoretical curve; if the modulus of elasticity in tension were assumed to be slightly below 10.8×10^6 psi. the tensile strains would also correlate. In view of the consistency noted in Figures XXI, XXII, XXIV, XXV, and XXVI, the authors are inclined to think that this might actually be the case.

the Gaskell-Jenkins interface, and is depicted [illegible].

Maximum Stress

[illegible] those rims which were intentionally distorted are [illegible] gages were fixed at points of maximum (0^o and 180^o) and minimum (90^o and 270^o) diameters. The strains at 0^o and 180^o were averaged and plotted for rings No. 3-9 on the right side of figures 11 - 14. Similarly, the average of the 60^o and 120^o readings are shown on the left side of the same plots. The theoretical curve is simply a plot of equation (3) with $\cos 2\theta$ equal to plus or minus one and $p = p_{max.} = 0.320$. The strains at 0^o and 180^o are pertinently important in that they are normally used in the fabrication of a coiltube [illegible]; consequently, the stresses at these positions are given added consideration.

With the exception of rings No. 3 and 4, the correlation of measured and theoretical stress is entirely satisfactory. On the pressure basis the conservative [illegible] within a range of ± 5-1/2 [illegible] of the theoretical curve; this was the assumed [illegible] factor. The tensile stress [illegible] below the [illegible] curve; it [illegible] to be slightly [illegible] than [illegible] mostly flat portion. [illegible] the small [illegible] to Figures 11, 12, 13, and 14, the [illegible] inclined to [illegible].

In a sense Rings No. 3 and 6 were special cases. As pointed out Ring No. 3 appeared to be the dividing line between configurations in which the two lobe out-or roundness pattern predominated and those which were affected by variations in thickness, harmonics, and/or local irregularities such as a small dent or gouge. Figure XX shows clearly that the measured strains were considerably below the predicted values up to a pressure of 400 psi; at this point the measured strains literally jumped to the theoretical curve. Figure XX tends to substantiate the remarks made previously; that is, in practical cases of out-of-roundness a two lobe configuration derived simply and directly may allow prediction of strains of acceptable accuracy at sufficiently high pressures, but further work is required before complete justification is obtained.

Figure XXIII shows merely that measured strains for Ring No. 6 were larger than the predicted strains over the entire range of pressures. The consistency lends some doubt to the authors' contention that the test may have been faulty.

In conjunction with the considerations of circumferential strain distribution, the results above indicate quite clearly that equation (3) is valid within the qualifications of the derivation; this conclusion is based upon the behavior of

In a series Ring No. 3 and 6 mils of cast copper. As pointed out Ring No. 1 appeared to be yielding in a pattern predominated and those which were elastic, variations in thickness, ramparts, and/or local irregularities as a small dent or bump. Figure XX shows clearly that the measured strains were considerably below the predicted values up to a pressure of 400 psi; at this point the measured strains literally jumped to the theoretical curve. Figure XX tends to substantiate the theories made previously: that is, in practical cases of out-of-roundness a two lobe configuration develops at low and directly may allow prediction of strains of more tangible concern at sufficiently high pressures, but further work is required before complete justification is obtained.

Figure XXIII shows nearly that measured strains for Ring No. 6 were larger than the predicted strains over the entire range of pressures. The conclusion may have been to the authors' conviction that this test may have been result?

In conjunction with the comparisons of circumferential strain distribution, the results above indicate quite clearly that equation (3) -a more refined version of the derivation; this comment [illegible]

Rings No. 4, 5, 7, 8, and 9 in which the assumption of a configuration $R_o + u_o \cos 2\theta$ was obviously justified.

Collapse Pressure

Figure XXVII shows the collapse pressures of the nine rings plotted versus the ratio of out-of-roundness to average thickness and serves to identify the points shown on Figure XXVIII. The single curve is a plot of equation (4) with σ_{max} = 35,000 psi. Figure XXVIII is more informative in that several variations of equation (4) are plotted; the values of σ_{max} and h which apply to each curve are indicated in the legend.

Foregoing results (see Figure V) indicate that Rings No. 1 and 2 did not assume a two lobe configuration until the ring was in the process of failing completely; if a stable two lobe pattern existed it was possible over a very small range of pressure. Regardless of the cause of the random strain distribution, Figure XXVIII demonstrates clearly that the failure of Rings No. 1 and 2 could have been predicted by equation (4) in which σ_{max} is 41,000 psi and $h = h_{min.} = 0.243"$.

There are two ways in which to view these results. First, it would appear that the minimum thickness, u_o as measured, and the point at which the stress-strain curve departs significantly from linearity are the only factors

Rings No. 4, 5, 7, 8, and 9 to which the assumption of a configuration R_0 + No one 2 e was obviously justified.

Collapse Pressure

Figure XXVII shows the collapse pressures of the nine rings plotted versus the ratio of out-of-roundness to average thickness and again identify the points shown on Figure XXVIII. The single curve is a plot of equation (4) with q_{max} = 23,000 psi. Figure XXVIII is more informative in that several variations of equation (4) are plotted; the values of q_{max} and n which apply to each curve are indicated in the l-egend.

Corresponding results (see Figure V) indicate that Rings No. 1 and 2 did not assume a two lobe configuration until the ring was in the process of failing completely; it is stable two lobe pattern existed it was possible over a very small range of pressure. Regardless of the cause of the random strain distribution, Figure XVIII demonstrates clearly that the failure of Rings No. 1 and 2 could have been predicted by equation (4) to within q_{max} is 21,000 psi and n = $n_{min.}$ = 0.0275.

There are two ways in which [illegible] deprive significantly from linearity are the [illegible] measured, and the point at which the strain [illegible] first. It would appear that [illegible] , by se-

to be considered; hence, the use of equation (4) would be justified. This line of reasoning would infer that previous remarks relative to the importance of the basic two lobe configuration are entirely correct and that in practical cases of out-of-roundness one could neglect out-of-round other than that indicated by a simple consideration of diameters. On the other hand it is possible to reason that the variation in thickness was actually not significant; this statement could be based upon the collapse pressure of Rings No. 3, 4, and 5. Then the occurrence of collapse below the predition based upon average thickness would be explained in terms of stress introduced by a superimposed but undetected configuration or by local irregularities. The authors can conclude only that in this case of practical out-or-roundness and arbitrary strain distribution the collapse was predicted by equation (4) using minimum thickness and σ_{max} = 41,000 psi.

Rings No. 3, 4, and 5 differed from Rings No. 1 and 2 in that a clearly defined cosine type strain distribution was observed before failure. In each case the strain peaks corresponded to peaks in the out-of-roundness plot. Furthermore, the progressive failure which occurred in these rings may be contrasted to the rather sudden collapse of Rings No. 1 and 2.

to be considered; hence, the use of equation (4) would be
justified. This line of reasoning would infer that previous
remarks relative to the importance of the basic two load
conditions are entirely correct and that in practical
cases of out-of-roundness one could neglect out-of-round
other than that indicated by a simple consideration of
diameters. On the other hand it is possible to reason that
the variation in thickness was actually not significant;
this statement could be based upon the collapse pressure
of Rings No. 3, 4, and 5. Then the occurrence of collapse
below the prediction based upon average thickness would be
explained in terms of stress introduced by a superimposed
but undetected configuration or by local irregularities.
The authors can conclude only that in this case of practical
out-of-roundness and arbitrary strain distribution the
collapse was predicted by equation (4) using minimum thickness
and q_{max} = 41,000 psi.

Rings No. 3, 4, and 5 differed from Rings No. 1 and 2
in that a clearly defined plastic strain distribution
was observed before failure. In each case the strain gage
corresponded to peaks in the out-of-roundness plot. Furthe-
more, the pre-existing plastic moment occurred in these rings
may be considered by the rather modest collapse of Rings
No. 1 and 2.

Figure XXVIII shows that Rings No. 3, 4, and 5 collapsed at pressures very near to predictions given by equation (4) with σ_{max} = 41,000 psi and h = h_{ave}. These results seem to justify the argument above that the variation in thickness in itself was not significant and that the behavior of Rings No. 1 and 2 should be explained on the basis of harmonics and/or local irregularities. Nevertheless, the authors' only conclusion is that for rings of u_o/h from 0.10 to 0.30 equation (4), when used with the stress at which marked departure from linearity occurs, will predict quite accurately the failures in those rings where an initial configuration of $R_o + u_o \cos 2\theta$ is predominate.

Rings No. 7, 8, and 9 collapsed at pressures consistently above the predicted collapse pressure. Furthermore, stable configurations were obtained in which the maximum compressive stress was considerably above the yield point. Obviously as u_o increases, the criteria used in computing the collapse pressure becomes more conservative. This result is explained by the fact that the hoop stress upon which the bending stress is superimposed was less at the time yielding occurred in the outer fibers; in addition, the change in stress with respect to pressure was also less in the rings of greater u_o when this yielding began. Then to obtain instability in rings of greater out-of-roundness a larger increase in

Figure XXVIII shows that Rings No. 3, 4, and 5 collapsed at pressures very near to predictions given by equation (4) with σ_{max} = 41,000 psi and n = $n_{s/s}$. These results seem to justify the argument above that the variation in thickness in Rings No. 1 and 2 should be explained on the basis of harmonics and/or local irregularities. Nevertheless, the author's only conclusion is that for rings of M_0/h from 0.13 to 0.30 equation (4) when used with the stress at which marked departure from linearity occurs will predict quite accurately the failures in those rings where an initial configuration of M_0 + M_0 cos 2 θ is predominate.

Rings No. 7, 8, and 9 collapsed at pressures consistently above the predicted collapse pressure. Furthermore, elastic configurations were obtained in which the maximum compressive stress was considerably above the yield point. Obviously as M_0 increases, the criteria used in computing the critical pressure becomes more conservative. This result is explained by the fact that the hoop stress upon the bending stress is superimposed was less at the time yielding occurred in the outer fibers; in addition, the change in stress with respect to pressure was also less in the rings of greater

pressure was required beyond the point of initial yield in the outer fibers. The authors conclude that for values of u_o/h greater than 0.30 and less than 1.10 the predicted collapse pressures are somewhat conservative but would be considered satisfactory for usual engineering design.

pressure was required beyond the point of initial yield in the outer fibers. The authors conclude that for values of ν_o/h greater than 0.30 and less than 1.10 the predicted collapse pressures are somewhat conservative but would be considered satisfactory for usual engineering design.

V.

CONCLUSIONS

1. The properties of aluminum alloy 61S-T6 were particularly well adapted to the objectives of this thesis.
2. The most significant problem encountered in the method of experimentation was the reduction of friction at the gasket-Plexiglas interface.
3. The relation for predicted strains in thin rings, equation (3), is valid when the assumed configuration, $R_o + u_o \cos 2\theta$, is obtained.
4. In those cases where the equation for predicted strains is valid and the value of h/D is 0.0285 a failure criteria based upon the stress level in the outer fibers predicts quite accurately the collapse of thin rings in which u_o/h is between 0.10 and 0.30. For values of u_o/h between 0.30 and 1.10 the criteria is somewhat conservative but not to an extent which would be considered over-cautious in engineering design.
5. From the general trend of the experimental collapse pressures as u_o/h decreases, the authors conclude that the collapse pressure predicted for perfectly circular rings by the Levy Formula, $P_{crit} = \frac{3EI}{R^3}$, is valid.

V.

CONCLUSIONS

1. The properties of aluminum alloy 618-T6 were particularly well adapted to the objectives of this thesis.

2. The most significant problem encountered in the method of experimentation was the reduction or friction at the basket-flexible interface.

3. The relation for predicted stress in thin rings, equation (3), is valid when the assumed configuration, $R_o + w_o \cos 2\theta$, is obtained.

4. In those cases where the equation for predicted stress is valid and the value of M/S is 0.005 a failure criteria based upon the stress level in the outer fibers predicts quite accurately the collapse of thin rings in which w_o/h is between 0.10 and 0.30. For values of w_o/h between 0.20 and 1.10 the criteria is somewhat conservative but not to an extent which would be considered over-conservative in applying design.

5. From the general trend of the experimental collapse pressures vs w_o/h factors it is evident that the collapse pressure predicted by the Timoshenko formula, $p_{cr} = \frac{E}{4}\left(\frac{h}{R}\right)^3$, is very

VI.

RECOMMENDATIONS

1. Aluminum alloy 61S-T6 should be used in any extension of the experimentation described in this thesis.
2. A thorough, quantitative investigation of the friction at the gasket-Plexiglas interface should precede any further use of a test apparatus such as that described herein.
3. An investigation should be made for the purpose of determining the effect of deviations from a basic two lobe pattern as measured in this thesis. The rings to be investigated should be of constant thickness and the initial configuration should be known precisely.
4. A series of rings, machined as circular as possible and to a close tolerance in thickness, should be tested in order to further substantiate the Levy Formula.
5. It is recommended that the scope of this experimentation be extended to include commercial shapes such as I or H sections.

VI.

RECOMMENDATIONS

1. Aluminum alloy 618-T6 should be used in any extension of the experimentation described in this thesis.

2. A thorough, quantitative investigation of the fracture at the Bakelite-Plexiglas interface should precede any further use of a test specimen such as that described herein.

3. An investigation should be made for the purpose of determining the effect of deviations from a basic two hole pattern as measured in this thesis. The trips to be investigated should be of constant thickness and the initial configuration should be known precisely.

4. A series of trips, machined as circular as possible and to a close tolerance in thickness, should be tested in order to further substantiate the Levy formula.

5. It is recommended that the scope of this experimentation be extended to include commercial shapes such as I or H sections.

VII.

A P P E N D I X

APPENDIX

AII.

APPENDIX A

Details of Procedures

Selection of Material for Construction of Rings

Initially the authors considered the possibility of using steel in the manufacture of the rings. A length of centrifugally cast steel tubing of 18" outside diameter and 1-3/4" wall thickness was available. However, the expense of constructing a test apparatus to accommodate steel rings was considered prohibitive in view of the uncertainty of the results. Furthermore, it was felt that the visual test chamber made possible through the use of Plexiglas would be of tremendous advantage during the test phase; this innovation was not considered feasible in the preliminary design of an apparatus to accommodate the pressures necessary to collapse steel rings.

The use of plastics was also given consideration. The various types of plastics were gradually eliminated for one or more of the following reasons:

1. The relatively low modulus of plastics resulted in very low predicted collapse pressures.
2. The ultimate strength was generally low relative to available metals.
3. The extent of a linear stress-strain relationship was limited.

APPENDIX A

Details of Procedures

Selection of Material for Construction of Rings

Initially the authors considered the possibility of using steel in the manufacture of the rings. A length of centrifugally cast steel tubing of 10" outside diameter and 1-3/4" wall thickness was available. However, the expense of constructing a test apparatus to accommodate steel rings was considered prohibitive in view of the uncertainty of the results. Furthermore, it was felt that the visual test chamber made possible through the use of flexible would be of tremendous advantage during the test phase; this innovation was not considered feasible in the preliminary design of an apparatus to accommodate the pressure necessary to collapse steel rings.

The use of plastics was also given consideration. The various types of plastics were thoroughly investigated for one or more of the following reasons:

1. The relatively low modulus of plastics resulted in very low [illegible] pressures.
2. The ultimate strength [illegible] to the relative to available metal.
3. The extent of plastic [illegible] in resistance was limited.

These considerations indicated that the range of pressures over which useful data could be obtained was very limited, and, further, that the accuracy of the results would be questionable unless extreme precautions were taken in instrumentation.

As noted in Section II, aluminum alloy 61S-T6 appeared to satisfy the requirements of moderate collapse pressures, an essentially linear stress-strain relationship over a considerable range of stresses, and availability.

Manufacture of Rings

As pointed out in Section II the aluminum alloy tubing as received was cut into lengths several times the intended width of the test rings. Alternatively, the rings could have been machined to final dimensions. However, it is rather doubtful that the edges of the finished ring would have remained planar after the ring had been subjected to deformation in a loading machine and a heat treatment. A ring warped in this manner would tend to bind against the plane sides of the annular test chamber within the test apparatus. Consequently, the machining of the rings to the specified width was scheduled as the last operation in the manufacturing process.

The heat treatment of the aluminum alloy was accomplished by the Forge Shop, Boston Naval Shipyard. Specifically, the

These considerations indicated that the range of pressures over which useful data could be obtained was very limited, and, further, that the accuracy of the results would be questionable unless extreme precautions were taken in instrumentation.

As noted in Section II, aluminum alloy 61S-T6 appeared to satisfy the requirements of moderate collapse pressures, an essentially linear stress-strain relationship over a considerable range of stresses, and availability.

Manufacture of Rings

As pointed out in Section II the aluminum alloy tubing as received was cut into lengths several times the intended width of the test rings. Alternatively, the rings could have been machined to final dimensions. However, it is rather doubtful that the edges of the finished ring would have remained planar after the ring had been subjected to deformation in a loading machine and a heat treatment. A ring warped in this manner would tend to find contact the plane sides of the annular test chamber making the test apparatus. Consequently, the machining of the rings to the specified width was scheduled as the last operation in the manufacturing process.

The heat treatment of the [illegible] was accomplished by the Rocky Shop, Boston Naval Shipyard. Specified the

solution heat treatment consisted of a two hour soaking period at 970° F followed by a rapid quench in hot water at 180°F. The hot water quench was specified as an additional precaution against residual stresses. Actually the danger of residual stresses was not particularly significant in view of the rather thin thickness of alloy being quenched; nevertheless, the precaution was considered worthwhile since a hot water quench does not reduce the tensile properties appreciably below those obtainable with a cold water quench. The quench was followed by a precipitation heat treatment at 350°F for eight hours. The characteristics of aluminum alloy 61S-T6 as given in reference (5) are:

Tensile Strength	45,000 psi.
Yield Strength	40,000 psi.
E, Young's Modulus	10×10^6 psi.

Upon inspection of the sections after the heat treatment, it was found that the magnitude of the out-of-roundness introduced had not changed by any significant amount.

Instrumentation

The requirements placed upon the type strain gage selected were that the gage be small enough for mounting in the space available and that the gage length be sufficiently short with respect to the strain gradient. The SR-4, type A-7, strain gage satisfied these requirements. The gages

solution heat treatment consisted of a two hour soaking period at 970° F followed by a rapid quench in hot water at 180°F. The hot water quench was specified as an additional precaution against residual stresses. Actually the danger of residual stresses was not particularly significant in view of the rather thin sections of alloy being quenched; nevertheless, the precaution was considered worthwhile since a hot water quench does not reduce the tensile properties appreciably below those obtainable with a cold water quench. The quench was followed by a precipitation heat treatment at 350°F for eight hours. The characteristics of aluminum alloy 618-T6 as given in reference (5) are:

Tensile Strength 45,000 psi.

Yield Strength 40,000 psi.

E, Young's Modulus $10x10^6$ psi.

Upon inspection of the sections after the heat treatment, it was found that the magnitude of the out-of-roundness introduced had not changed by any significant amount.

Instrumentation

The requirements placed upon the [illegible] selected were that the gage be small enough [illegible] the space available and that the gage length be sufficiently short with respect to the strain gradient. The chief type A-7, strain gage satisfied these requirements. The [illegible]

could be easily mounted within the width of the ring, and, furthermore, a 3/16" gage length was entirely adequate since the predicted stress gradient in the vicinity of points of maximum stress was very small.

A multiple selector switchbox was used to facilitate reading the strain indications. The switchbox was constructed to permit the operator to set the same initial reading on all strain gages.

Design and Manufacture of Test Apparatus

The primary concern of the authors in the initial design of a test apparatus was the application of a uniform pressure on the outer surface of the rings without the introduction of restraining forces on the ring edges. An annular test chamber appeared to be the most suitable in this respect. The annulus was designed such that the tolerance between the surfaces and the edges of the ring would be exceedingly small, i.e., order of 0.001-0.002". This would facilitate sealing and yet the ring would remain "free floating" so to speak. From preliminary calculations based on the Levy formula for the collapse of 9" diameter aluminum rings or the 1/4 inch thickness, it was estimated that the test chamber would be subjected to a pressure of approximately 500 psi. Because Plexiglas is beautifully clear and can be obtained in large thick sheets with polished surfaces, it was decided to design the test annulus with upper and

could be easily removed within the width of the rims, and, furthermore, a 3/16" gage length was entirely adequate since the predicted stress gradient in the vicinity of points of maximum stress was very small.

A multiple selector switchbox was used to facilitate reading the strain indications. The switchbox was constructed to permit the operator to set the zero initial reading on all strain gages.

Design and Manufacture of Test Apparatus

The primary concern of the authors in the initial design of a test apparatus was the application of a uniform pressure on the outer surface of the rims without the introduction of restraining forces on the rim edges. An annular test chamber appeared to be the most suitable in this respect. The annulus was designed such that the tolerance between the surfaces and the edges of the ring would be exceedingly small, i.e., order of 0.001-0.002". This would facilitate sealing and yet the ring would remain "free floating" so to speak. From preliminary calculations based on the Lamé formula for the collapse of 8" diameter annulus rings of the 1/4 inch thickness, it was estimated that the test chamber would be subjected to a pressure of approximately 500 psi. Because Plexiglas is beautifully clear and can be obtained in large tube sheets with polished surfaces, it was decided to design the test annulus with clear Plexi-

lower surfaces of this material. This construction would permit visual inspection of collapse and the possibility of obtaining deflection readings. Plexiglas, however, has a low modulus of elasticity and therefore required backing to prevent the surface from deflecting appreciably when subjected to the expected pressures. The top steel web assembly and the bottom steel reinforcing ring as indicated in Figure I were designed for limiting the deflections of the Plexiglas. The hole in the bottom Plexiglas and reinforcing plates was introduced to accommodate strain gage leads. The steel surfaces indicated to be surface ground in Figure I were so designated to provide good contact surfaces between the steel and the Plexiglas. The steel surfaces as received, particularly those of the spacer ring, would not have insured a uniform spacing of the two surfaces forming the annulus.

Although four 3/8" bolts would have been sufficient from considerations of strength alone, it was decided to use sixteen in order to obtain oil tightness.

Originally rubber gasket material was to be used between the spacer ring and the Plexiglas surfaces to prevent oil leakage at the junction of the steel and Plexiglas outside the annulus. However, the rubber gasket would have been compressed in varying amounts around the test apparatus,

depending on the tension in each bolt upon tightening up. It was possible to circumvent this difficulty by using paper of 0.010" thickness.

The pressure tap was designed to accommodate a 1/4" copper tube fitting. The air release tap diametrically opposite was so placed to vent the test chamber while oil was being introduced.

The cathetometer used to take deflection readings was mounted as indicated in Figure II and Photograph No. (4). The heavy brass plug on which the cathetometer is mounted was machined to fit snugly into the thick walled pipe which had been welded into the center of the top web assembly of the test apparatus; the thick-walled pipe was machined true to an axis perpendicular to the surface of the Plexiglas. A bench mark was established on the web assembly to facilitate taking deflection readings.

Proof Test of Apparatus

The objective of this phase of the testing was to solve as completely as possible the many unexpected problems of detail which plague any initial effort. In addition it was desirable to establish a standard test procedure to be used during the remainder of the experimental work.

Of concern to the authors during the design of the

apparatus was the need for an effective seal between the Plexiglas surfaces and the edges of the test ring. Preliminary considerations indicated that the most likely solution would be the use of either a leather or rubber gasket of slightly greater width than the ring. The gasket could be shaped to fold back against the Plexiglas surface when the top assembly was bolted down. See Figure XXIX (a). To facilitate assembly, the gasket could be glued to the outer circumference of the ring prior to insertion in the test chamber.

The following trial gaskets were selected for preliminary investigation:

1. A strip of bicycle tire inner tube cut to 3/4" width, 28" in length, and joined at the ends with rubber cement. Results: Not successful because a secure junction could not be obtained.
2. Rubber electrical tape applied to the outer circumference with the ends lapped.
   Results: Extrusion of the tape between the Plexiglas surfaces and the edges of the ring occurred at pressures of about 400 psi.
3. Leather strip 3/4" wide, 28" in length with junction secured by a special leather cement.
   Results: Not successful because the strengtn of the junction was unsatisfactory.

apparatus was the need for an effective seal between the Plexiglas surfaces and the edges of the test rims. Preliminary considerations indicated that the most likely solution would be the use of either a leather or rubber gasket of slightly greater width than the rims. The gasket could be shaped to fold back against the Plexiglas surface when the top assembly was bolted down. See Figure XXIX (a). To facilitate assembly, the gasket could be glued to the outer circumference of the rims prior to insertion in the test chamber.

The following trial gaskets were selected for preliminary investigation:

1. A strip of bicycle tire inner tube cut to 3/4" width, 25" length, and joined at the ends with rubber cement. Results: Not successful because a secure junction could not be obtained.

2. Rubber electrical tape applied to the outer circumference with the ends taped.
Results: Extrusion of the tape between the Plexiglas surfaces and the edges of the rims occurred at pressures of about 400 psi.

3. Leather strip 3/4" wide, 25" in length with ends secured by a small leather rivet.
Results: Not successful because the creation of the junction was unsatisfactory.

FIGURE XXIX

DETAILS OF GASKET

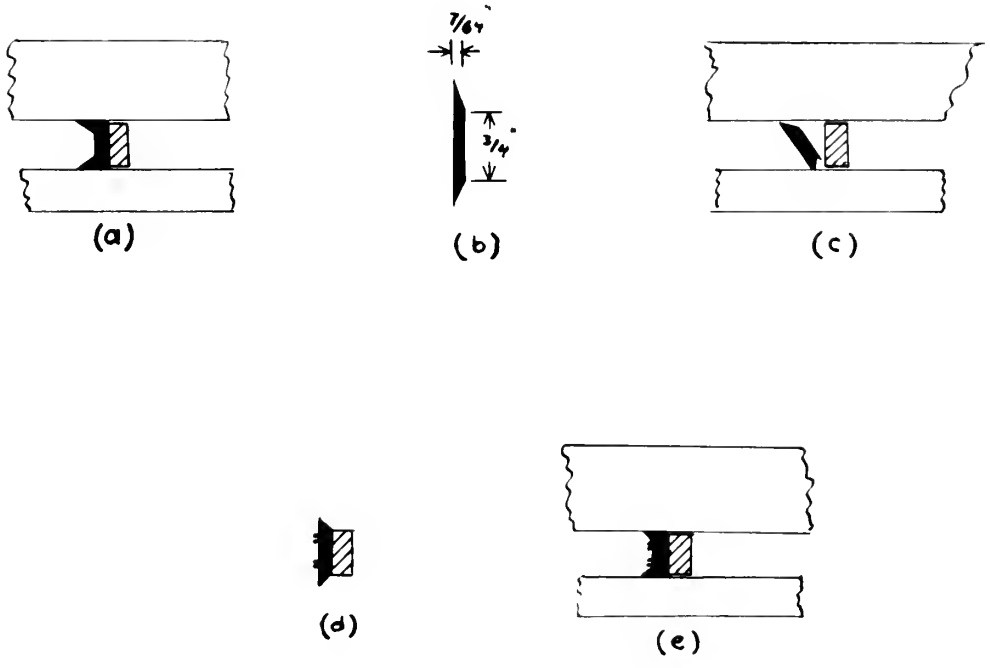

FIGURE XXX

DETAILS OF LUBRICANT TEST

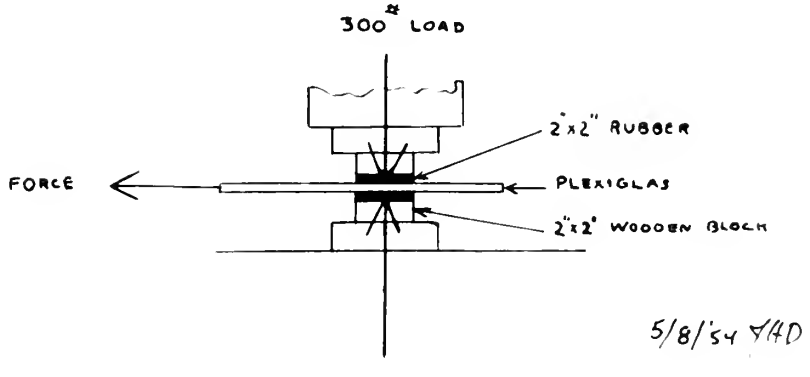

5/8/'54 AHD

4. Truck tire inner tube 9" in diameter cut to 3/4" width with edges beveled as indicated in Figure XXIX(b).

   Results: Successful in holding pressures up to 875 psi.; it is interesting to note that even at this pressure the gasket did not extrude. Pressure was not increased beyond 875 psi. for fear of introducing a permanent set in the top Plexiglas surface. There was no junction difficulty in this particular case because the gasket was continuous.

Further experimentation with gasket No. 4 indicated that the 3/4" width was unnecessary and could be reduced to 1/2". The angle of the bevel was changed to 45°. The procedure for cutting the final gaskets was as follows:

1. Glue a 2" section of rubber tubing around the circumference of an 11" wooden disk attached to a lathe chuck.
2. Place the disk in the lathe and turn at slow speeds. (At high speeds the rubber was torn loose from the wooden disk)
3. Hold a sharp, pointed cutting tool at 45° to the edge of the disk and slowly press the tool into the rubber in much the same manner as if turning down wood.

4. After the cutting blade has passed completely through the rubber, the tool is removed and inserted 1/2" from the first cut, the inclination being that required to produce a reverse 45° bevel.

Gaskets manufactured as above were glued to the outer circumference of the preliminary test rings with clear or black rubber cement. It was thought that a film of oil between the rubber gasket and the Plexiglas surfaces would be sufficient to lubricate the gasket and permit relatively friction free slipping. The first preliminary test ring was placed in the test chamber. Pressures well above the predicted failure pressure were applied without collapse of the ring. The possibility of passing through the first critical collapse pressure was discounted as a complete explanation because without noticeable restraint such could occur only by a combination of ideal conditions and fortuitious circumstances. The apparatus was repeatedly opened to adjust the gasket and, if possible to determine the cause of the restraint. After numerous trials the ring buckled at approximately 550 psi., well above the predicted collapse pressure.

The second preliminary test ring was similarly tested several times without success. At this point the authors

decided to direct all efforts toward the elimination of the restraining force which prevented the collapse of the rings at reasonable pressures. It was assumed that the restraining force occurred as a result of friction between the rubber gasket and the Plexiglas since without the gasket the rings were found to be completely free when enclosed in the test chamber.

Several types of lubricants were investigated by spreading the lubricant over two rubber 2"x2" squares and sandwiching a piece of Plexiglas between them. A load was applied to the rubber squares by means of wooden blocks placed between the rubber squares and the heads of a loading machine. See Figure XXX. The force necessary to move the Plexiglas under specified loads was observed. The following lubricants were used:

1. Number 40 S.A.E. motor oil.

   Results: Plexiglas could not be moved by a force less than 40 lbs. when a load of 300 lbs. was applied by the loading machine.

2. Silicone Compound DC4.

   Results: Same as No. 1.

3. Vaseline

   Results: Plexiglas could be moved by a force of approximately 8 lbs. when a load of 300 lbs. was applied by the loading machine.

4. Clear rubber cement applied to rubber and oil film on Plexiglas.

   Results: Plexiglas could be moved by a force of approximately 6 lbs. when a load of 300 lbs. was applied by the loading machine.

5. Black rubber-to-metal cement applied to rubber and oil film on Plexiglas.

   Results: Lubricant effective to the extent that the 2" rubber squares would not remain in place under wooden blocks as the load was being applied.

On the basis of the preceding results it was concluded that the black rubber-to-metal cement was the most suitable lubricant. The rubber gasket was cemented to the outer circumference of the preliminary test ring with a large amount of cement. The aluminum ring was then placed in the test apparatus and the top assembly bolted in position. It was noted at this time that the gasket would not remain in position on the aluminum ring but pulled away in the manner indicated in Figure XXIX (c). The top assembly was removed and several strands of light string were passed around the outer circumference of the gasket. See Figure XXIX (d). The beveled edges were observed to fold back uniformily along the surface of the Plexiglas when the ring and gasket were again placed in the test chamber and the top assembly had been positioned and bolted down. See Figure XXIX (e).

Pressure was applied and the preliminary test ring buckled very close to the predicted collapse pressure.

The test procedure with respect to gasket material, gasket size, and lubrication was thus established. It is worthwhile to note that the best results were obtained when the black cement was applied to the beveled surfaces, the inner surface of the gasket, and the outer surface of the ring. The cement was allowed to dry slightly after application.

In an effort to obtain deflection readings the authors considered testing the rings in two phases. During the first phase clear rubber cement would be used as the lubricant and both deflection readings and strain readings were to be recorded up to the pressure at which collapse was expected. The pressure would then be released and the ring removed for lubrication with the black cement. During the second phase strain readings were to be taken until actual collapse occurred. However, as pointed out previously strains taken during the two phases did not correlate. Furthermore, the cathetometer proved impractical. The third preliminary test ring was strain gaged and tested with various lubricants and gasket material to show that the strains did in fact depend upon these factors. Results of these tests were presented in Figure IV.

of these tests were previously [illegible].

the strain dry [illegible] upon these [illegible]. [illegible]
with various [illegible] the gasket material [illegible]
The third preliminary test cell was [illegible]
relate. Furthermore, the deformations [illegible]
atously strains taken during the two phases [illegible]
actual collapse occurred. However, as [illegible]
the second phase strain readings were to be taken multi-
ring removed for inspection with the [illegible]. During
was expected. The procedure would then be released an. the
were to be recycled up to the pressure at which collapse
Impulsat and both deflection readings and strain readings
first phase clear rubber cement would be used as the
considered testing the rings in two phases. During the
In an effort to obtain deflection readings the authors
sation.

ring. The cement was allowed to dry slightly after appli-
inner surface of the gasket, and the other surface of the
the clear cement was applied to the beveled surfaces, the
worthwhile to note that the best results were obtained when
gasket size, and insertion was then completed. It is

The test procedure with respect to gasket material
very close to the predicted collapse pressure.
Pressure was applied and the preliminary test ring buckled

During the proof testing period oil leakage around the bolt holes was noted. A strip of rubber electrical tape 3/4" in width was glued to the inner circumference of the spacer ring. The edges of this seal folded back toward the center of the test chamber and were pressed tightly against the Plexiglas when pressure was applied. Holes were cut in the electrical tape in way of the pressure tape and air release tape. Little or no oil leakage was observed around the bolt holes throughout the remainder of the tests.

Test of Compression Specimens

Since the value of E, Young's Modulus, and σ_y were of primary importance in the correlation of experimental data with predicted stress distribution and collapse pressure, it was immediately apparent to the authors that the values of E and σ_y for the material used should be determined experimentally rather than relying on handbook values which represent average data at best.

Four 2 1/2" wide semi-circular sections were cut from the original piece of aluminum tubing to provide the material from which tensile specimens were to be machined. The semi-circular sections had to be flattened before machining; therefore, the sections were annealed prior to the flattening process to prevent cracking. Annealing was carried out as recommended by the Metals Handbook (5). To insure a reasonably complete anneal, the semi-circular

During the proof testing period oil leaks around the
bolt holes were noted. A strip of rubber electrical tape
3/4" in width was glued to the inner circumference of the
spacer ring. The edges of this seal folded back toward the
center of the test chamber and were pressed tightly against
the flexiglas when pressure was applied. Holes were cut in
the electrical tape in way of the pressure taps and the
release tape. Little or no oil leakage was observed around
the duplex holes throughout the remainder of the tests.

Test of Compression Specimens

Since the value of κ, Young's Modulus, and σ_y were
of primary importance in the correlation of experimental
data with predicted stress distribution and collapse pressure,
it was immediately apparent to the authors that the values
of E and σ_y for the material used should be ascertained
permanently rather than relying on handbook values that
represent average data at best.

Four 2 1/2" wide semi-circular sections were cut from
the original piece of Lucite tubing to obtain the
material from which tensile specimens were machined.
The semi-circular specimens were to be flattened before
machining; therefore, no sections were cut from the
circumferential regions of greatest thickness. Specimen
configuration is recommended by the Materials Division
of the National Bureau of Standards, the specimen

sections were heated for two hours at 750°F, then slowly cooled (not faster than 50°F per hour) until a temperature of 500° was reached. Below 500°F the rate or cooling was not important and the sections were removed from the furnace and allowed to air cool to room temperature.

The sections were then flattened in a mechanical press. No difficulties were experienced in the flattening operation. Cracks did not occur in the sections and very little spring-back was observed when the upper head of the press was lifted from the sections. From all indications, the aluminum alloy was sufficiently annealed by the process described above.

To obtain uniformity of physical properties in the flattened sections, they were heat treated along with the ring sections as described in the material related to the manufacture of the rings.

Unfortunately the flat bar specimens were not quite as true as the authors had anticipated, and it was feared that appreciable bending stresses might be introduced in the tensile specimens during the application of loads. Initial unfairness could have been eliminated by machining the flat surfaces; however, this procedure would not have been too practical since the original wall thickness of the aluminum tubing was only 0.250". A further reduction in thickness would have increased the difficulty of mounting

of Tensometers. It was then decided to use three compression specimens cut from the flattest portions of the section. Since the length of the specimens required was of the order of 2.5", no appreciable difficulty was experienced in finding planar portions of the sections for this purpose.

Three compression specimens were manufactured by the Department of Mechanical Engineering machine shop.
Specification for compression test specimens:

Using the same material from which the rings were manufactured, three specimens are to be cut and milled to the dimensions of 0.84 x 2.53 inches, these dimensions conforming to the proportions of 1 to 3 as recommended by ASTM standards.

The compression specimen test block and two Type A Huggenberger Tensometers were furnished by the Department of Mechanical Engineering, M.I.T. Load was applied to the block by means of a 10,000 pound capacity loading machine.

As recommended by the Metals Handbook, the Tensometers were mounted on opposite sides of the test specimen. The gage points were located symmetrically with respect to the middle of the length of the specimen and not closer to the end of the specimen than a distance approximately equal to the width of the specimen.

It was found necessary to reset the Huggenberger Tensometers at least four times during each specimen run.

APPENDIX B

Sample Calculations and Summary of Data

Calculation of R_o, Radius to Outer Circumference

The radius to the outer circumference of each ring was measured indirectly by fitting a wire of known diameter around the outer surface of the ring, scribing the wire in position, and then measuring the distance between the scribe marks on a 36" rule.

Then $R_o = \frac{\ell}{2\pi} - d$, where

R_o = radius to outer circumference of the ring in inches.

ℓ = length of wrapper wire measured between scribe marks in inches.

d = diameter of wrapper wire in inches.

Thus for Ring No. 1:

$$R_o = \frac{28.391}{2\pi} - 0.01"$$

$$R_o = 4.509"$$

The value of R_o used in the remaining calculations is the average of all measured radii.

Compression Test

The strains given by opposite Huggenberger Tensometers at a specified load were averaged to avoid errors due to bending. The stress corresponding to this strain was obtained by dividing the load by the original cross sectional area of the specimen.

The following calculation applies in the case of Specimen No. 1 at a load of 4500 lbs.

Data - Specimen No. 1

Load lbs.	Huggenberger No. 2201 Calibration Factor 1040 Rdg.	Rdg	Rdg	Huggenberger No. 2195 Calibration Factor 1051 Rdg	Rdg	Rdg
0	1.50			1.5		
500	1.30	-0.20	-0.20	1.24	-0.26	-0.26
1000	1.09	-0.21	-0.41	1.00	-0.24	-0.30
1500	0.86	-0.23	-0.64	0.74	-0.26	-0.76
2000	0.63	-0.23	-0.87	0.50	-0.24	-1.00
2500	0.43	-0.20	-1.07	0.28	-0.22	-1.22
3000	0.20	-0.23	-1.30	0.05	-0.23	-1.45
Reset	1.50			1.50		
3500	1.33	-0.17	-1.47	1.28	-0.22	-1.67
4000	1.11	-0.22	-1.69	1.04	-0.24	-1.91
4500	0.89	-0.22	-1.91	0.81	-0.23	-2.14

$$\text{Strain} = \frac{\text{Tensometer Reading}}{\text{Calibration Factor}} \text{ in inches/inch}$$

ε_1 = Strain in inches/inch given by Tensometer No. 2201

ε_2 = Strain in inches/inch given by Tensometer No. 2195

ε = Average measured strain in micro-inches/inch

$$\varepsilon_1 = \frac{-1.91}{1040} = -0.001836 \text{ inches/inch}$$

$$\varepsilon_2 = \frac{-2.14}{1051} = -0.002036 \text{ inches/inch}$$

$$\varepsilon = \frac{(-0.001836) + (-0.002036)}{2} \times 10^6 = -1936 \text{ micro-inches/inch}$$

$$\sigma = \frac{L}{txw}$$

σ = stress in psi.

L = load in lbs.

t = thickness of specimen in inches

w = width of specimen in inches

$$\sigma = \frac{4,500}{(0.201)(0.841)} = 20,500 \text{ psi}$$

The results of the Compression Test calculations are presented as experimental points in Figure III.

Circumferential Strains

Except for the case of Ring No. 2 all predicted circumferential strain distributions were computed directly from equation (3).

$$\epsilon = \frac{P R_o}{E h} + \frac{6 P R u_o h \cos 2\theta}{Eh^3 - 4 P R^3}$$

All factors are defined in SYMBOLS AND ABBREVIATIONS, page vi. For Ring No. 7, $u_o = 0.1535"$; then for P = 240 psi.

$$\epsilon = \frac{(240)(4.508)}{(0.250)(10.8 \times 10^6)} + \frac{(6)(240)(4.383)(0.1535)(0.250)\cos 2\theta}{(10.8 \times 10^6)(0.250)^3 - (4)(240)(4.383)^3}$$

$\epsilon = (400.7) + (2754.8 \cos 2\theta)$ micro-inches/inch

θ	$\cos 2\theta$	$2754.8 \cos 2\theta$	ϵ
0° & 180°	+1	+2754.8	+3155.5
30° & 210°	+1/2	+1377.4	+1778.1
60° & 240°	-1/2	-1377.4	-976.7
90° & 270°	-1	-2754.8	-2354.1
120° & 300°	-1/2	-1377.4	-976.7
150° & 330°	+1/2	+1377.4	+1778.1

Since ε has been defined as a compression strain the plotted values become:

Circumferential Position	Strain in micro-inches/inch
0° & 180°	-3155.5
30° & 210°	-1788.1
60° & 240°	+976.7
90° & 270°	+2354.1
120° & 300°	+976.7
150° & 330°	-1778.1

The circumferential strain distribution for Ring No. 2 was computed using the measured out-of-roundness at each station instead of $u_o \cos 2\theta$.

$$\varepsilon = \frac{P R_o}{E h} + \frac{6 P R u h}{Eh^3 - 4PR^3} \qquad (5)$$

Data:

Circumferential Position	u	Sign as determined by equation (5)
0° & 180°	0.0075"	-
30° & 210°	0.0800"	+
50° & 230°	0.0125"	+
80° & 260°	0.0065"	+
110° & 290°	0.0045"	-
150° & 330°	0.0125"	-

at P = 400 psi.

Since E was left defined as a compression strain the [illegible]

values become:

Circumferential location	Strain in micro-inch-c/in-c
0^o & 180^o	-3155.5
30^o & 210^o	-1788.1
60^o & 240^o	+979.7
90^o & 270^o	+2324.1
120^o & 300^o	+970.7
150^o & 330^o	-1776.1

The circumferential strain distribution for mins No. 2 was

computed using the measured cat-ol-roundness at section

instead of $w_o \cos 2\theta$.

$$\epsilon = \frac{1}{E}\frac{R_o}{h} + \frac{c}{w^2 - 4R^2}\frac{E\,R\,w\,h}{} \qquad (5)$$

Data:

Circumferential location	Strain as determined by equation (5)
0^o & 180^o	0.0795"
30^o & 210^o	0.0800"
60^o & 240^o	0.0125"
90^o & 270^o	0.0005"
120^o & 300^o	-0.0245"
150^o & 330^o	-0.0425"

at r = 400 mm.

$$\varepsilon = \frac{(400)(4.508)}{(0.250)(10.8 \times 10^6)} + \frac{(6)(400)(4.383)(0.250)\,u}{(10.8 \times 10^6)(0.250)^3 - (4)(400)(4.383)^3}$$

ε = 667.85 + 83353.4 u micro-inches/inch

Substituting data:

Circumferential Position	Plotted Strain in micro-inches/inch
0° & 180°	-42.7
30° & 210°	-1334.65
50° & 230°	-1709.77
80° & 200°	-1209.03
110° & 290°	-292.76
150° & 330°	+374.08

A summary of all such calculated values is given in the form of curves, see Figures V, VIII, XI, XIV, and XVII.

Maximum Strains

The maximum strains at specified pressures were computed using equation (3). Cos 2 θ becomes +1 for 0° and 180° positions and -1 for 90° and 270° positions.

$$\varepsilon = \frac{P R_o}{E h} + \frac{6 P R u_o h}{E h^3 - 4PR^3} \qquad (6)$$

$$\varepsilon = \frac{P R_o}{E h} - \frac{6 P R u_o h}{E h^3 - 4 P R^3} \qquad (7)$$

ε for a ring of given u_o is computed from equations (6) and (7) at several increments of pressure. For Ring No. 5, u_o = 0.070"; then at 50 psi.:

ε at 0° and 180°

$$\varepsilon = \frac{(50)(4.508)}{(10.8 \times 10^6)(0.250)} + \frac{(6)(50)(4.383)(0.070)(0.250)}{(10.8 \times 10^6)(0.250)^3 - (4)(50)(4.383)^3}$$

ε = 234.9 micro-inches/inch (Plotted with - sign)

ε at 90° and 270°

$$\varepsilon = \frac{(50)(4.508)}{(10.8 \times 10^6)(0.250)} - \frac{(6)(50)(4.383)(0.070)(0.250)}{(10.8 \times 10^6)(0.250)^3 - (4)(50)(4.383)^3}$$

ε = - 68.0 micro-inches/inch (Plotted with + sign)

Pressure psi.	Plotted value at 0° and 180°	Plotted value at 90° and 270°
50	-234.9	+68.0
100	-507.7	+173.8
150	-834.3	+333.5
200	-1,241.7	+573.9
250	-1,778.1	+943.4
300	-2,539.9	+1,538.2
350	-3,750.7	+2,582.1
400	-6,077.3	+4,741.7

A summary of all such calculated values is given in the form of plots, see Figures XX-XXVI.

Collapse Pressures

The curves of predicted collapse pressures were derived indirectly by first plotting equation (4). Stresses at various pressures were computed for several values of u_o.

ε at 0^{o} and 180^{o}

ε = $\frac{(50)(4.506)}{(10.8 \times 10^{6})(0.250)}$ + $\frac{(0)(50)(4.363)(0.070)(0.250)}{(10.8 \times 10^{6})(0.250)^{3}-(4)(50)(4.363)^{3}}$

ε = 274.9 micro-inches/inch (plotted with - sign)

ε at 90^{o} and 270^{o}

ε = $\frac{(50)(4.506)}{(10.8 \times 10^{6})(0.250)}$ - $\frac{(0)(50)(4.363)(0.070)(0.250)}{(10.8 \times 10^{6})(0.250)^{3}-(4)(50)(4.363)^{3}}$

ε = -624.0 micro-inches/inch (plotted with - sign)

Pressure psi.	Plotted value at 0^{o} and 180^{o}	Plotted value at 90^{o} and 270^{o}
50	-1,134.9	-418.0
100	-2,047.7	-173.6
150	-2,854.3	+339.3
200	-3,541.7	+871.3
250	-4,177.1	+943.4
300	-4,525.5	+1,339.2
350	-3,730.7	+2,241.1
400	-4,077.3	+2,411.7

A summary of all such computations is given in Table XX-XXVI.

Conclusions from Measurements

The curves in Figure [illegible] indicate that [illegible]

[illegible] of Plots, and Magnitude [illegible]

A cross curve of predicted collapse pressures was then drawn using the values given by the intersection of a single ordinate 35,000 psi. or 41,000 psi. with the curves of stress versus pressure.

To compute one point for stress-pressure curves:

$u_o = 0.050"$, $P = 50$ psi., $h = 0.250"$

$$\sigma = \frac{P R_o}{h} + \frac{6 P R u_o h E}{E h^3 - 4 PR^3}$$

$$\sigma = \frac{(50)(4.508)}{(0.250} + \frac{(6)(50)(0.050)(4.383)(0.250)(10.8 \times 10^6)}{(10.8 \times 10^6)(0.250)^3 - (4)(50)(4.383)^3}$$

$\sigma = 2,090$ psi., maximum compressive stress

Similarly:

Pressure psi.	σ psi.
100	4,431
200	10,609
250	15,005
300	21,139
350	30,737
400	50,206

Values for $\sigma_{max.}$ were computed at several increments of pressure for the following values of u_o: 0.050", 0.100", 0.150", 0.200", and 0.250". The procedure was repeated using $h = h_{min.} = 0.243"$.

The results of these computations are presented as curves, Figure XXXI. Shown in the same Figure are ordinates

A cross curve of predicted collapse pressure was then drawn using the values given by the intersection of a single ordinate 35,000 psi. or 47,000 psi. with the curves of stress versus pressure.

To compute one point for sheet-pressure curves:

n_o = 0.050", I = 50 ksi., n = 0.250"

$$\sigma = \frac{P R_o}{h} + \frac{6 I R n_o h E}{h^3 - 4 I R^3}$$

$$\sigma = \frac{(50)(4.959)}{(0.250)} + \frac{(6)(50)(0.250)(4.709)(0.250)(10.8 \times 10^6)}{(10.8 \times 10^6)(0.250)^3 - (4)(50)(4.709)^3}$$

σ = 2,090 psi., maximum compressive stress

Similarly:

Pressure psi.	σ psi.
100	4,431
200	10,009
250	15,[illegible]
300	21,139
350	36,737
400	50,250

Values for $\sigma_{max.}$ [illegible] pressure for the following [illegible] 0.150", 0.200", [illegible] using h = $h_{min.}$ = 0.252".

The results of these computations are shown in curves, Figure XVII. Above [illegible] a tangent

FIGURE XXXI

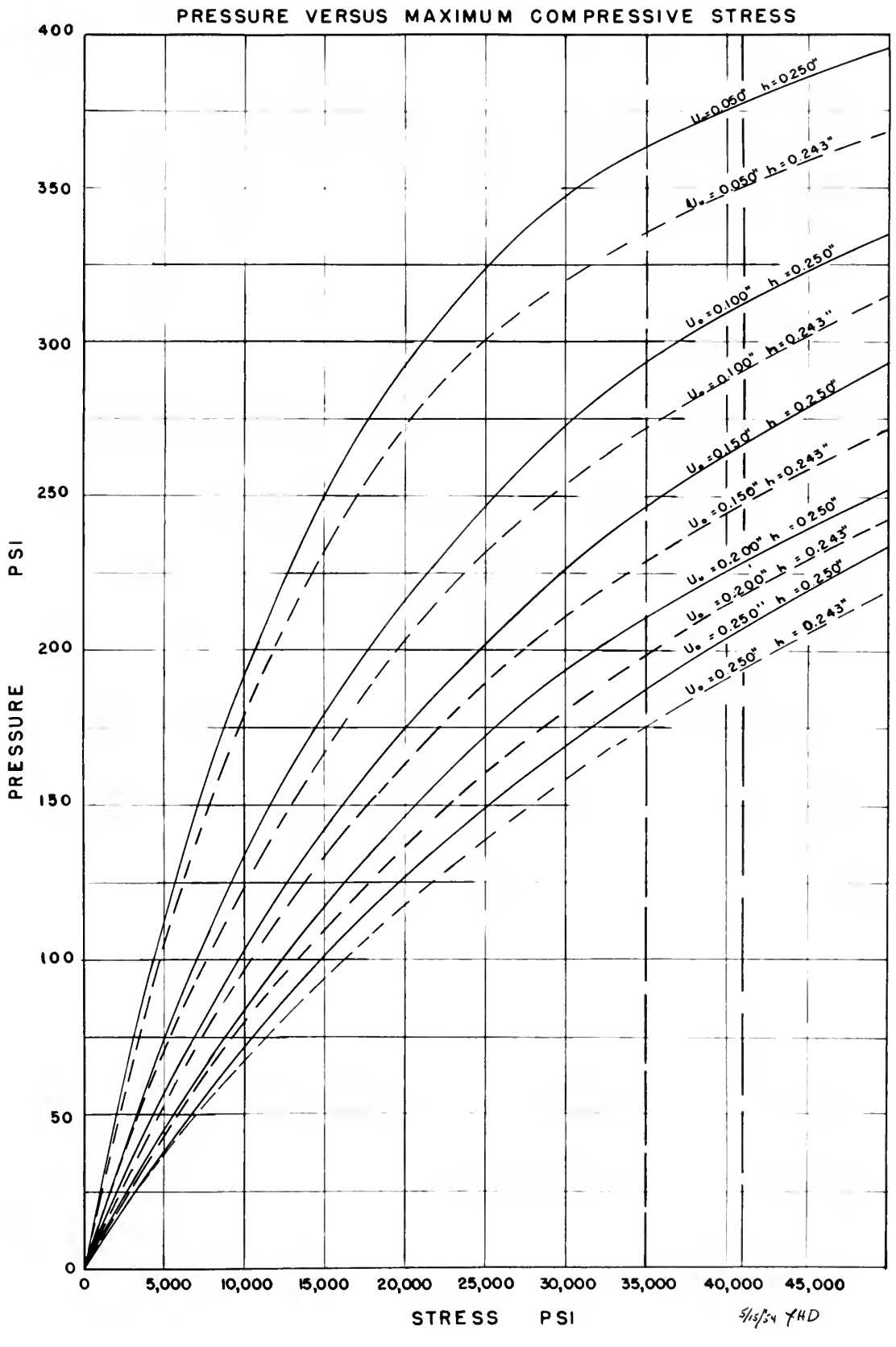
PRESSURE VERSUS MAXIMUM COMPRESSIVE STRESS
PRESSURE PSI
400
350
300
250
200
150
100
50
0
0
5,000
10,000
15,000
20,000
25,000
30,000
35,000
40,000
45,000
STRESS PSI
U_o=0.050" h=0.250"
U_o=0.050" h=0.243"
U_o=0.100" h=0.250"
U_o=0.100" h=0.243"
U_o=0.150" h=0.250"
U_o=0.150" h=0.243"
U_o=0.200" h=0.250"
U_o=0.200" h=0.243"
U_o=0.250" h=0.250"
U_o=0.250" h=0.243"
5/15/54 YHD

at 35,000 psi. and 41,000 psi. The intersection of pressure-stress curve with these ordinates determined the points through which the predicted collapse pressure curves were drawn; see Figures XXVII and XXVIII.

Experimental Strain Readings

The strain data was checked for significant errors by plotting measured strains versus pressure for each strain gage. There were no marked deviations from the fair curves which were drawn through the points. These curves were also used to determine the experimental points shown in the plots of circumferential strain distribution in Figures V, VIII, XI, XIV, and XVII.

The measured values of strain shown in Figures IV and XX-XXVI were taken directly from the original data.

APPENDIX C

Original Data

Table I is a tabulation of the data taken during the test of the three compression specimens.

Table II is a record of the data recorded during the investigation of the effects of lubricants and gasket material upon the strain distribution around the inner circumference of the aluminum rings.

Tables III - XI contain data relating to physical dimensions, circumferential strain distribution, collapse pressures and diametral readings for each ring.

APPENDIX C

Original Data

Table I
Data for Stress-Strain Curve in Compression

Load	Specimen #1		Specimen #2		Specimen #3	
lbs.	H#2201	H#2195	H#2201	H#2195	H#2201	H#2195
0	1.50	1.50	1.60	1.58	1.58	1.60
500	1.30	1.24				
1000	1.09	1.00	1.40	0.94	1.26	0.95
1500	0.86	0.74				
2000	0.63	0.50	0.96	0.41	0.82	0.55
2500	0.43	0.28				
3000	0.20	0.05	0.59	0.03	0.37	0.19
Reset to	1.50	1.50	1.55	1.62	1.59	1.49
3500	1.33	1.28				
4000	1.11	1.04	1.05	1.15	1.15	1.06
4500	0.89	0.81				
5000	0.66	0.57	0.62	0.69	0.70	0.60
5500	0.45	0.35	0.45	0.52	0.46	0.35
6000	0.21	0.10	0.22	0.29	0.24	0.10
Reset to	1.50	1.60	1.60	1.55	1.54	1.53
6500	1.30	——	1.36	1.30	1.40	1.43
7000	1.05	——	1.10	1.03	1.11	1.18
7500	0.82	——	0,90	0.80	0.78	0.84
8000	0.56	——	0.65	0.55	0.38	0.40
				Reset to	1.50	1.50
8500	0.25	——	0.35	0.19	1.10	1.07
Reset to	1.50	1.50	1.50	1.60		
9000	1.01	1.12	1.34	1.40	0.11	-0.12
				Reset to	1.47	1.55
9110					0.29	0.10
9500	0.01	0.30	0.54	0.36		
Reset to	1.50	1.50	1.55	1.45		
9630	0.02	0.23				
9650			0.39	-0.15		

| | | |

Table II
Strain Data for Preliminary Test Ring

Lubricant #2 Gasket #1 — Strains in Micro-inch per inch at Positions indicated

Pressure psi	0°	30°	60°	90°	120°	150°	180°	210°	240°	270°	300°	330°
0	7000	7000	7000	7000	7000	7000	7000	7000	7000	7000	7000	7000
99	6820	6920	——	6800	6695	6800	6890	6900	6830	6875	6780	——
200	6615	6830	——	6600	6375	6580	6765	6800	6660	6750	6570	——
303	6375	6800	——	6385	5920	6270	6660	6790	6580	6630	6215	——
403	6120	7650	——	6190	5200	5690	6510	7010	6780	6540	5630	——

Lubricant #1 Gasket #1

Pressure psi	0°	30°	60°	90°	120°	150°	180°	210°	240°	270°	300°	330°
0	7000	7000	7000	7000	7000	7000	7000	7000	7000	7000	7000	7000
99	6770	6900	——	6815	6680	6760	6855	6890	6850	6885	6765	——
200	6530	6870	——	6650	6285	6460	6700	6840	6770	6785	6480	——
303	6270	7100	——	6400	5500	5875	6635	7055	6860	6610	5870	——

Lubricant #1 Gasket #2

Pressure psi	0°	30°	60°	90°	120°	150°	180°	210°	240°	270°	300°	330°
0	7000	7000	7000	7000	7000	7000	7000	7000	7000	7000	7000	7000
99	6760	6880	——	6850	6700	6760	6840	6880	6860	6905	6790	——
200	6520	6810	——	6670	6350	6500	6700	6800	6735	6800	6550	——
303	6260	6840	——	6460	5840	6120	6550	6820	6730	6695	6150	——
403	6070	7430	——	6150	4810	5305	6450	7345	7180	6540	7240	——

Table III
Dimensions and Strain Data for Ring #1

Angle	h in.	b in	Strains in micro-inches per inch at pressures indicated: 0	99	200	303	403	453
0°	0.247	0.444	11,000	10,780	10,610	10,500	10,270	10,120
30°	0.250	0.445	11,000	10,805	10,670	10,515	10,285	10,160
60°	0.253	0.445	11,000	10,850	10,680	10,460	10,305	10,215
90°	0.261	0.444	11,000	10,860	10,640	10,370	10,200	10,120
120°	0.261	0.445	11,000	10,820	10,590	10,310	10,090	9,970
150°	0.256	0.444						
180°	0.247	0.445	11,000	10,860	10,790	10,790	10,730	10,710
210°	0.242	0.446	11,000	10,830	10,750	10,670	10,545	10,460
240°	0.243	0.445	11,000	10,805	10,560	10,255	9,910	9,730
270°	0.243	0.444	11,000	10,800	10,480	10,120	9,830	9,715
300°	0.246	0.444	11,000	10,870	10,700	10,530	10,470	10,430
330°	0.248	0.445	11,000	10,840	10,705	10,605	10,530	10,460

Collapse Pressure = 450 psi

Outside Radius = 4.509"

Diameter readings in inches

0-180°	9.012	90-270°	9.038
15-195°	9.008	105-285°	9.035
30-210°	9.008	120-300°	9.031
45-225°	9.016	135-315°	9.032
60-240°	9.027	150-330°	9.033
75-255°	9.035	165-345°	9.026

Table IV

Dimensions and Strain Data for Ring #2

Angle	h in.	b in.	Strains in micro-inches per inch at pressures indicated 0	99	200	303	403
0°	0.244	0.448	11,000	10,820	10,690	10,590	11,670
30°	0.246	0.447	11,000	10,810	10,605	10,320	9,550
60°	0.249	0.448	11,000	10,780	10,520	10,100	8,030
90°	0.247	0.448	11,000	10,765	10,475	10,090	8,640
120°	0.250	0.448	11,000	———	———	———	———
150°	0.252	0.448	11,000	10,800	10,580	10,250	8,850
180°	0.261	0.448	11,000	10,885	10,770	10,755	11,160
210°	0.262	0.448	11,000	10,850	10,750	10,840	12,335
240°	0.256	0.448	11,000	10,825	10,650	10,555	10,930
270°	0.247	0.448	11,000	10,920	10,885	11,040	12,720
300°	0.243	0.448	11,000	10,905	10,840	10,895	12,030
330°	0.243	0.448	11,000	10,790	10,540	10,220	9,580

Collapse Pressure = 425 psi

Diameter readings in inches.

0–180°	9.020	90–270°	9.042
15–195°	9.030	105–285°	9.027
30–210°	9.050	120–300°	9.020
45–225°	9.060	135–315°	9.013
60–240°	9.057	150–330°	9.010

Outside radius = 4.510"

Table V
Dimensions and Strain Data for Ring #3

Angle	h in.	b in	Strains in micro-inches per inch at pressures indicated						
			0	99	200	303	353	403	423
0°	0.246	0.444	9,000	8,745	8,450	7,940	7,690	6,225	5,230
30°	0.249	0.443	9,000	8,730	8,385	7,830	7,550	6,280	6,080
60°	0.249	0.445	9,000	8,840	8,640	8,475	8,390	8,450	9,150
90°	0.251	0.444	9,000	8,950	8,960	9,130	9,240	9,480	11,360
120°	0.254	0.443	9,000	8,895	8,840	8,930	8,980	9,040	10,010
150°	0.261	0.444	9,000	8,815	8,640	8,460	8,360	8,180	7,520
180°	0.262	0.445	9,000	8,750	8,460	8,035	7,775	7,405	5,760
210°	0.256	0.445	9,000	8,770	8,490	8,070	7,830	7,530	6,410
240°	0,247	0.444	9,000	8,840	8,660	8,490	8,410	8,355	8,860
270°	0.243	0.445	9,000	8,940	8,940	9.060	9,110	9,370	11,220
300°	0.243	0.445	9,000	8,755	8,520	8,360	8,410	8,660	9,920
330°	0.244	0.445	9,000	8,850	8,735	8,650	8,570	8,280	7,530

Collapse Pressure = 430 psi.

Diameter readings in inches.

Outside Radius = 4.510"

0-180°	9.072	90-270°	8.965
15-195°	9.071	105-285°	8.986
30-210°	9.061	120-300°	9.007
45-225°	9.041	135-315°	9.032
60-240°	9.017	150-330°	9.047
75-255°	8.983	165-345°	9.064

Table VI

Dimensions and Strain Data for Ring #4

Angle	h in.	b in	Strains in micro-inches per inch at pressures indicated 0	99	150	200	252	303	353	378
0°	0.261	0.445	7,000	6,670	6,460	6,170	5,720	5,140	4,260	3,340
30°	0.254	0.446	7,000	6,765	6,600	6,410	6,140	5,800	5,340	4,910
60°	0.251	0.446	7,000	6,900	6,850	6,855	6,925	7,090	7,420	7,810
90°	0.246	0.444	7,000	7,080	7,170	7,350	7,670	8,180	9,025	9,950
120°	0.249	0.444	7,000	6,880	6,860	6.880	6,955	7,110	7,425	7,820
150°	0.246	0.444	7,000	6,740	6,600	6,390	6,115	5,700	5,105	———
180°	0.244	0.445	7,000	6,630	6,400	6,045	5,580	4,900	3,900	———
210°	0.244	0.445	7,000	6,720	6,550	6,340	6,090	5,770	5,390	———
240°	0.245	0.445	7,000	6,950	6,940	7,015	7,150	7,470	8,000	———
270°	0.248	0.444	7,000	7,120	7,215	7,420	7,690	8,205	7,980	———
300°	0.255	0.444	7,000	6,855	6,790	6,775	6,760	6,820	6,950	———
330°	0.262	0.444	7,000	6,710	6,570	6,345	6,100	5,680	5,135	———

Collapse Pressure = 383 psi

Outside Radius = 4.506"

Diameter readings in inches

0-180°	9.102	90-270°	8.910
15-195°	9.099	105-285°	8.953
30-210°	9.069	120-300°	9.006
45-225°	9.028	135-315°	9.047
60-240°	8.986	150-330°	9.075
75-255°	8.940	165-345°	9.097

Table VI

Diagnoses and Status for Dept. for Girls ***

Table VII

Dimensions and Strain Data for Ring #5

Angle	h	b	Strains in micro-inches per inch at pressures indicated								
	in.	in.	0	49	99	150	200	252	303	328	353
0°	0.244	0.444	9,000	8,910	8,625	8,290	7,880	7,390	6,630	6,120	5,250
30°	0.243	0.441	9,000	8,870	8,650	8,400	8,100	7,750	7,260	6,960	6,455
60°	0.243	0.444	9,000	8,860	8,860	8,880	8,930	9,030	9,280	9,495	9,880
90°	0.247	0.445	9,000	9,020	9,175	9,415	9,720	10,140	10,800	11,245	12,100
120°	0.256	0.445	9,000	8,925	8,890	8,890	8,925	9,000	9,170	9,295	9,580
150°	0.262	0.444	9,000	8,875	8,695	8,470	8,210	7,900	7,470	7,200	6,760
180°	0.261	0.443	9,000	8,850	8,605	8,260	7,860	7,360	6,650	6,200	5,380
210°	0.253	0.445	9,000	8,900	8,710	8,470	8,215	7,880	7,430	7,130	7,595
240°	0.250	0.445	9,000	8,930	8,910	8,920	8,960	9,030	9,200	9,320	9,590
270°	0.248	0.444	9,000	8,955	9,100	9,330	9,600	9,990	10,625	11,060	11,905
300°	0.249	0.44 5	9,000	8,900	8,885	8,915	8,965	9,075	9,320	9,530	9,965
330°	0.247	0.445	9,000	8,920	8,765	8,560	8,340	8,090	7,710	7,485	7,115

Collapse Pressure = 365 psi.

Diameter readings in inches

Outside Radius = 4.508"

0-180°	9.138	90-270°	8.856
15-195°	9.122	105-285°	8.923
30-210°	9.097	120-300°	8.994
45-225°	9.046	135-315°	9.041
60-240°	8.985	150-330°	9.086
75-255°	8.920	165-345°	9.122

TABLE VIII

[illegible]

| | | |

Table VIII
Dimensions and Strain Data for Ring #6

Angle	h in	b in	Strains in micro-inches per inch at pressures indicated 0	49	99	150	200	252	303
0°	0.244	0.444	9,000	8,740	8,460	8,105	7,580	6,850	5,580
30°	0.243	0.445	9,000	8,780	8,560	8,290	7,945	7,475	6,725
60°	0.244	0.445	9,000	8,960	8,950	8,970	9,080	9,290	9,770
90°	0.244	0.445	9,000	9,155	9,340	9,610	10,035	10,690	11,860
120°	0.248	0.445	9,000	8,990	8,990	9,020	9,120	9,315	9,760
150°	0.249	0.445	9,000	8,830	8,600	8,340	8,005	7,540	6,825
180°	0.247	0.445	9,000	8,720	8,390	7,975	7,445	6,670	5,305
210°	0.252	0.445	9,000	8,840	8,685	8,490	8,240	7,885	7,310
240°	0.257	0.445	9,000	8,995	9,015	9,075	9,200	9,410	9,890
270°	0.261	0.445	9,000	9,100	9,230	9,430	9,770	10,330	11,410
300°	0.260	0.444	9,000	8,990	8,980	9,010	9,115	9,330	9,860
330°	0.253	0.444	9,000	8,870	8,705	8,520	8,280	7,950	7,410

Collapse Pressure = 345 psi.

Outside Radius = 4.506"

Diameter readings in inches

0-180°	9,158	90-270°	8.858
15-195°	9.134	105-285°	8.908
30-210°	9.093	120-300°	8.986
45-225°	9.038	135-315°	9.042
60-240°	8.968	150-330°	8.910
75-255°	8.905	165-345°	9.142

Table XXII

Distribution of Land Holdings by Size and Tenure in Rural Areas

Size of holdings	Owned		Rented		Owned and rented	
	No.	Area	No.	Area	No.	Area
Below 1	1,000	500	1,000	500	1,000	500
1-2	2,000	1,500	2,000	1,500	2,000	1,500
2-3	3,000	2,500	3,000	2,500	3,000	2,500
3-4	4,000	3,500	4,000	3,500	4,000	3,500
4-5	5,000	4,500	5,000	4,500	5,000	4,500
5-6	6,000	5,500	6,000	5,500	6,000	5,500
6-7	7,000	6,500	7,000	6,500	7,000	6,500
7-8	8,000	7,500	8,000	7,500	8,000	7,500
8-9	9,000	8,500	9,000	8,500	9,000	8,500
9-10	10,000	9,500	10,000	9,500	10,000	9,500
10-11	11,000	10,500	11,000	10,500	11,000	10,500
11-12	12,000	11,500	12,000	11,500	12,000	11,500
12-13	13,000	12,500	13,000	12,500	13,000	12,500
13-14	14,000	13,500	14,000	13,500	14,000	13,500
14-15	15,000	14,500	15,000	14,500	15,000	14,500
15-16	16,000	15,500	16,000	15,500	16,000	15,500
16-17	17,000	16,500	17,000	16,500	17,000	16,500
17-18	18,000	17,500	18,000	17,500	18,000	17,500
18-19	19,000	18,500	19,000	18,500	19,000	18,500
19-20	20,000	19,500	20,000	19,500	20,000	19,500
20-21	21,000	20,500	21,000	20,500	21,000	20,500
21-22	22,000	21,500	22,000	21,500	22,000	21,500
22-23	23,000	22,500	23,000	22,500	23,000	22,500
23-24	24,000	23,500	24,000	23,500	24,000	23,500
24-25	25,000	24,500	25,000	24,500	25,000	24,500
25-26	26,000	25,500	26,000	25,500	26,000	25,500
26-27	27,000	26,500	27,000	26,500	27,000	26,500
27-28	28,000	27,500	28,000	27,500	28,000	27,500
28-29	29,000	28,500	29,000	28,500	29,000	28,500
29-30	30,000	29,500	30,000	29,500	30,000	29,500
30-31	31,000	30,500	31,000	30,500	31,000	30,500
31-32	32,000	31,500	32,000	31,500	32,000	31,500
32-33	33,000	32,500	33,000	32,500	33,000	32,500
33-34	34,000	33,500	34,000	33,500	34,000	33,500
34-35	35,000	34,500	35,000	34,500	35,000	34,500
35-36	36,000	35,500	36,000	35,500	36,000	35,500
36-37	37,000	36,500	37,000	36,500	37,000	36,500
37-38	38,000	37,500	38,000	37,500	38,000	37,500
38-39	39,000	38,500	39,000	38,500	39,000	38,500
39-40	40,000	39,500	40,000	39,500	40,000	39,500
40-41	41,000	40,500	41,000	40,500	41,000	40,500
41-42	42,000	41,500	42,000	41,500	42,000	41,500
42-43	43,000	42,500	43,000	42,500	43,000	42,500
43-44	44,000	43,500	44,000	43,500	44,000	43,500
44-45	45,000	44,500	45,000	44,500	45,000	44,500
45-46	46,000	45,500	46,000	45,500	46,000	45,500
46-47	47,000	46,500	47,000	46,500	47,000	46,500
47-48	48,000	47,500	48,000	47,500	48,000	47,500
48-49	49,000	48,500	49,000	48,500	49,000	48,500
49-50	50,000	49,500	50,000	49,500	50,000	49,500
50-51	51,000	50,500	51,000	50,500	51,000	50,500
51-52	52,000	51,500	52,000	51,500	52,000	51,500
52-53	53,000	52,500	53,000	52,500	53,000	52,500
53-54	54,000	53,500	54,000	53,500	54,000	53,500
54-55	55,000	54,500	55,000	54,500	55,000	54,500
55-56	56,000	55,500	56,000	55,500	56,000	55,500
56-57	57,000	56,500	57,000	56,500	57,000	56,500
57-58	58,000	57,500	58,000	57,500	58,000	57,500
58-59	59,000	58,500	59,000	58,500	59,000	58,500
59-60	60,000	59,500	60,000	59,500	60,000	59,500
60-61	61,000	60,500	61,000	60,500	61,000	60,500
61-62	62,000	61,500	62,000	61,500	62,000	61,500
62-63	63,000	62,500	63,000	62,500	63,000	62,500
63-64	64,000	63,500	64,000	63,500	64,000	63,500
64-65	65,000	64,500	65,000	64,500	65,000	64,500
65-66	66,000	65,500	66,000	65,500	66,000	65,500
66-67	67,000	66,500	67,000	66,500	67,000	66,500
67-68	68,000	67,500	68,000	67,500	68,000	67,500
68-69	69,000	68,500	69,000	68,500	69,000	68,500
69-70	70,000	69,500	70,000	69,500	70,000	69,500
70-71	71,000	70,500	71,000	70,500	71,000	70,500
71-72	72,000	71,500	72,000	71,500	72,000	71,500
72-73	73,000	72,500	73,000	72,500	73,000	72,500
73-74	74,000	73,500	74,000	73,500	74,000	73,500
74-75	75,000	74,500	75,000	74,500	75,000	74,500
75-76	76,000	75,500	76,000	75,500	76,000	75,500
76-77	77,000	76,500	77,000	76,500	77,000	76,500
77-78	78,000	77,500	78,000	77,500	78,000	77,500
78-79	79,000	78,500	79,000	78,500	79,000	78,500
79-80	80,000	79,500	80,000	79,500	80,000	79,500
80-81	81,000	80,500	81,000	80,500	81,000	80,500
81-82	82,000	81,500	82,000	81,500	82,000	81,500
82-83	83,000	82,500	83,000	82,500	83,000	82,500
83-84	84,000	83,500	84,000	83,500	84,000	83,500
84-85	85,000	84,500	85,000	84,500	85,000	84,500
85-86	86,000	85,500	86,000	85,500	86,000	85,500
86-87	87,000	86,500	87,000	86,500	87,000	86,500
87-88	88,000	87,500	88,000	87,500	88,000	87,500
88-89	89,000	88,500	89,000	88,500	89,000	88,500
89-90	90,000	89,500	90,000	89,500	90,000	89,500
90-91	91,000	90,500	91,000	90,500	91,000	90,500
91-92	92,000	91,500	92,000	91,500	92,000	91,500
92-93	93,000	92,500	93,000	92,500	93,000	92,500
93-94	94,000	93,500	94,000	93,500	94,000	93,500
94-95	95,000	94,500	95,000	94,500	95,000	94,500
95-96	96,000	95,500	96,000	95,500	96,000	95,500
96-97	97,000	96,500	97,000	96,500	97,000	96,500
97-98	98,000	97,500	98,000	97,500	98,000	97,500
98-99	99,000	98,500	99,000	98,500	99,000	98,500
99-100	100,000	99,500	100,000	99,500	100,000	99,500

Grand Total = 5,000,000

Table IX
Dimensions and Strain Data for Ring #7

Angle	h in.	b in	Strains in micro-inches per inch at pressures indicated 0	49	99	150	200	226	242	273	288
0°	0.252	0.444	9,000	8,695	8,160	7,510	6,700	6,230	5,890	4,920	3,775
30°	0.245	0.444	9,000	8,850	8,465	8,010	7,460	7,180	6,960	6,375	5,850
60°	0.244	0.443	9,000	9,020	9,130	9,280	9,550	9,735	9,880	10,300	10,655
90°	0.244	0.444	9,000	9,140	9,630	10,210	10,950	11,380	11,700	12,725	14,110
120°	0.245	0.444	9,000	8,990	9,110	9,260	9,500	9,660	9,770	10,150	10,450
150°	0.248	0.443	9,000	8,850	8,460	8,130	7,630	7,340	7,140	6,590	6,090
180°	0.249	0.444	9,000	8,685	8,090	7,460	6,635	6,140	5,790	4,760	3,510
210°	0.248	0.444	9,000	8,790	8,485	8,110	7,660	7,420	7,260	6,810	6,465
240°	0.252	0.444	9,000	9,010	9,150	9,290	9,570	9,750	9,900	10,355	10,780
270°	0.257	0.444	9,000	9,230	9,680	10,200	10,910	11,330	11,620	12,570	13,590
300°	0.262	0.443	9,000	8,985	9,130	9,295	9,560	9,710	9,815	10,210	10,575
330°	0.259	0.442	9,000	8,800	8,520	8,220	7,820	7,585	7,430	7,025	6,730

Collapse Pressure = 290 psi

Outside Radius = 4.508"

Diameter readings in inches.

0-180°	9.293	90-270°	8.679
15-195°	9.259	105-285°	8.793
30-210°	9.155	120-300°	8.929
45-225°	9.052	135-315°	9.067
60-240°	8.905	150-330°	9.168
75-255°	8.775	165-345°	9.265

Table XX

[illegible]

[illegible]	[illegible]	[illegible]	[illegible]	[illegible]	[illegible]	[illegible]	[illegible]	[illegible]	[illegible]	[illegible]	[illegible]
[illegible]	[illegible]	[illegible]	[illegible]	[illegible]	[illegible]	[illegible]	[illegible]	[illegible]	[illegible]	[illegible]	[illegible]

Table X

Dimensions and Strain Data for Ring #8

Angle	h in.	b in	Strains in micro-inches per inch at pressure indicated: 0	49	99	150	200	226	242	252
0°	0.263	0.445	9,000							
30°	0.260	0.444	9,000	8,660	8,240	7,690	6,935	6,570	6,250	5,940
60°	0.253	0.445	9,000	9,075	9,165	9,325	9,600	9,770	9,900	10,050
90°	0.250	0.445	9,000	9,400	9,930	10,635	11,580	12,200	12,705	13,260
120°	0.248	0.444	9,000	9,110	9,310	9,650	10,170	10,530	10,810	11,110
150°	0.249	0.445	9,000	8,730	8,440	8,100	7,620	7,360	7,185	7,040
180°	0.246	0.445	9,000	8,470	7,800	6,955	5,820	5,070	4,385	3,540
210°	0.244	0.445	9,000	8,680	8,260	7,710	7,040	6,630	6,330	6,050
240°	0.243	0.446	9,000	9,080	9,215	9,430	9,790	10,040	10,230	10,440
270°	0.244	0.445	9,000	9,440	10,010	10,775	11,810	12,520	13,110	13,860
300°	0.247	0.445	9,000	9,075	9,220	9,460	9,835	10,080	10,275	10,465
330°	0.257	0.444	9,000	8,675	8,310	7,835	7,240	6,870	6,585	6,320

Collapse Pressure = 257 psi

Outside Radius = 4.509"

Diameter readings in inches

0-180°	9,386	90-270°	8.571
15-195°	9.341	105-285°	8.686
30-210°	9.207	120-300°	8.847
45-225°	9.066	135-315°	9.026
60-240°	8.879	150-330°	9.167
75-255°	8.659	165-345°	9.286

Table XI
Dimensions and Strain Data for Ring #9

Angle	h in.	b in	Strains in micro-inches per inch at pressures indicated. 0	49	99	150	180	200
0°	0.248	0.443	9,000	8,290	7,425	6,260	5,380	4,560
30°	0.244	0.444	9,000	8,570	8,055	7,390	6,910	6,495
60°	0.244	0.444	9,000	9,150	9,395	9,780	10,120	10,410
90°	0.243	0.444	9,000	9,620	10,430	11,490	12,320	13,130
120°	0.244	0.443	9,000	9,190	9,435	9,820	10,140	10,420
150°	0.252	0.444	9,000					
180°	0.261	0.444	9,000	8,290	7,415	6,280	5,430	4,630
210°	0.261	0.445	9,000	8,640	8,220	7,670	7,285	6,960
240°	0.258	0.444	9,000	9,160	9,390	9,745	10,040	10,310
270°	0.251	0.445	9,000	9,570	10,310	11,275	12,025	12,750
300°	0.249	0.443	9,000	9,180	9,440	9,850	10,200	10,520
330°	0.250	0.443	9,000	8,650	8,215	7,645	7,260	6,930

Collapse Pressure = 220 psi

Outside Radius = 4.510"

Diameter readings in inches.

0-180°	9.532	90-270°	8.401
15-195°	9.452	105-285°	8.549
30-210°	9.254	120-300°	8.798
45-225°	9.021	135-315°	9.042
60-240°	8.794	150-330°	9.259
75-255°	8.575	165-345°	9.447

Table XI

Dimensions and Strength Data for Plug #2

Dimensions in micro-inches per inch at pressure indicated.

Angle	h	Zr	0	49	150	190	200
0°	0.0248	0.0000	0,000	1,425	6,250	6,340	6,560
30°	0.0244	0.0000	0,000	8,050	7,390	9,190	9,495
60°	0.0244	0.0000	0,000	9,340	9,780	10,120	10,420
90°	0.0243	0.0000	0,000	9,390	9,880	10,170	10,480
120°	0.0248	0.0000	0,000	9,390	9,880	10,170	10,480
150°	0.0252	0.0000	0,000	9,390	9,880	10,170	10,480
180°	0.0248	0.0000	0,000	9,390	9,880	10,170	10,480

Outside diameter = .250 bar

Original thickness = .020 inches

Original strength = 7,450 psi

Dimensions in microns.

Angle	h	Zr	0	49	150	190	200
0°	0.618	0.000	0,000	1,425	6,250	6,340	6,560
30°	0.618	0.000	0,000	8,050	7,390	9,190	9,495
60°	0.618	0.000	0,000	9,340	9,780	10,120	10,420
90°	0.618	0.000	0,000	9,390	9,880	10,170	10,480
120°	0.618	0.000	0,000	9,390	9,880	10,170	10,480
150°	0.618	0.000	0,000	9,390	9,880	10,170	10,480
180°	0.618	0.000	0,000	9,390	9,880	10,170	10,480

Outside diameter = 6.350 mm

Original thickness = .508 mm

Original strength = 51.36 kg/mm²

APPENDIX D

Literature Citations

(1) J. M. MONCRIEFF, "The Practical Column Under Central or Eccentric Loads", Transactions of the American Society of Civil Engineers, Vol. XLV, 1901, pp. 334-431.

(2) M. LEVY, "Buckling of Circular Rings and Tubes Under Uniform External Pressure", J. Math Pure et Appl. (Liouville), Vol. 10, No. 3, 1884, pp. 5.

(3) A. P. BORESI, Thesis submitted at University of Illinois, 1952.

(4) S. P. TIMOSHENKO, "Strength of Materials", Part II, Second Edition, August 1941, D. Van Nostrand Company, Inc., 250 Fourth Avenue, New York, pp. 101 - 103, 216 - 224.

(5) "Metals Handbook", 1948 Edition, pp. 109-111, 822.

(6) D. A. POLYCHRONE, "On the Buckling of Intermittently Supported Plates", Doctor of Science Thesis, M.I.T., 1949, pp. 64-73.

(7) M. L. PITTMAN and V. W. RINEHART, "On Providing Uniform Edge Compression Loads for Wide Flat Plates", N.A. Thesis, 1954.

APPENDIX D

Literature Citations

(1) M. CONFREY, "The Practical Design Under Uncertainty of Eccentric Joints", Transactions of the American Society of Civil Engineers, Vol. XIV, 1934, pp. 239-243.

(2) M. ISAY, "Buckling of Circular Rings and Tubes Under Uniform External Pressure", C. Math Phys ed. Petl. (Monville), Vol. 10, No. 1, 1934, pp. 3.

(3) A. P. BOZZOI, [illegible] of Mathematics, Clifton, 1953.

(4) S. P. TIMOSHENKO, "Strength of Materials", Part II, Second Edition, August 1941, D. Van Nostrand Company, 250 Fourth Avenue, New York, Pp. 103 -105, 1956.

(5) "Marks Handbook", [illegible] pp. 109-111, 1922.

(6) D. A. JOHNSONBOB, "On the Buckling of Inelastically Supported Plates", Doctor of Science Thesis, M.I.T., 1949, pp. 64-73.

(7) M. L. KITTNER and V. W. KINGSLAND, "On Improving Uniform Edge Compression Loads for Wide Flat Girder", T.A. Press, 1954.